CHESAPEAKE BAY INSTITUTE
The Johns Hopkins University

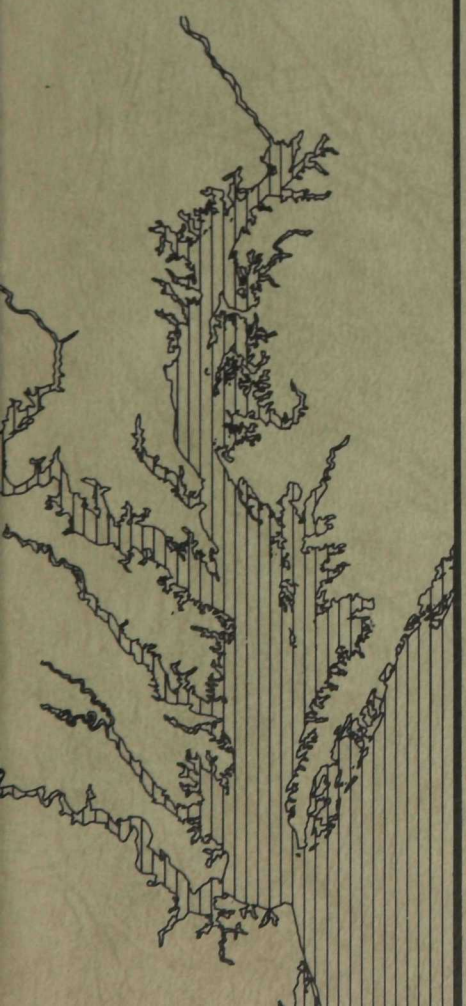

ON THE PREDICTION OF THE DISTRIBUTION OF EXCESS TEMPERATURE FROM A HEATED DISCHARGE IN AN ESTUARY

D. W. Pritchard
H. H. Carter

Technical Report 33

Reference 65-1 February 1965

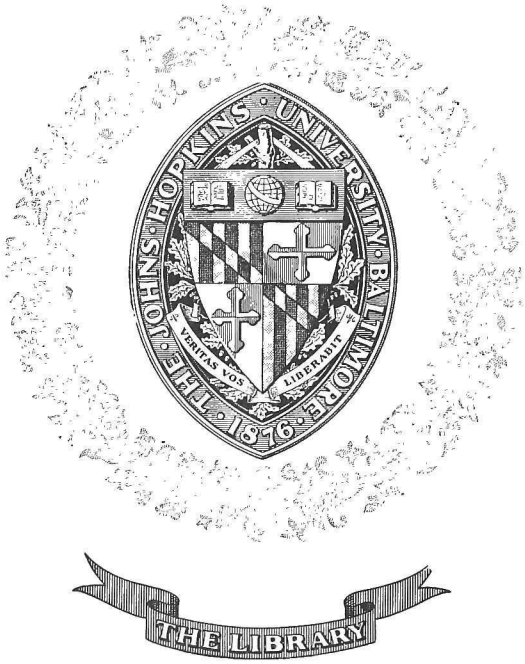
THE JOHNS HOPKINS UNIVERSITY BALTIMORE
VERITAS VOS LIBERABIT
1876
THE LIBRARY

CHESAPEAKE BAY INSTITUTE
THE JOHNS HOPKINS UNIVERSITY

ON THE PREDICTION OF THE DISTRIBUTION OF EXCESS TEMPERATURE FROM A HEATED DISCHARGE IN AN ESTUARY

D.W. Pritchard and H.H. Carter

TECHNICAL REPORT 33

This report contains results of work carried out for the Natural Resources Institute of the University of Maryland and for the United States Atomic Energy Commission (Contract AT(30-1)-3109).
NYO 10508

This report does not constitute final publication of the material presented.

Reference 65-1
February 1965

D.W. Pritchard
Director

TABLE OF CONTENTS

Page

Introduction 1

Field Study of Dispersion 4

Theoretical Considerations 6

Computation of the Probable Distribution of Excess Temperature . . 16

Appendix 35

The nonconservative processes of heat loss at the surface 35

Derivation of equation (4) 43

ILLUSTRATIONS

Figure		Page
1	Patuxent River estuary showing location of upstream and downstream cross sections. Insert shows immediate vicinity of PEPCO power plant with location of intake and outlet for cooling water	3
2	Ebb current U (kt) and peak dye concentration Γ_p (ppb) as a function of time during ebb tide at a section 3000 yd downstream from the discharge point, on the 15th tidal cycle after initiation of dye discharge	10
3	Characteristic concentration $\Gamma_d(t)$ as a function of time over the duration of the experiment, at a section 4000 yd downstream from release point	13
4	Observed dye distribution and predicted distribution of excess temperature at section 1000 yd downstream from release point, under steady-state conditions, during ebb tide	21
5	Observed dye distribution and predicted distribution of excess temperature at section 2000 yd downstream from release point, under steady-state conditions, during ebb tide	22
6	Observed dye distribution and predicted distribution of excess temperature at section 3000 yd downstream from release point, under steady-state conditions, during ebb tide	23
7	Observed dye distribution and predicted distribution of excess temperature at section 4000 yd downstream from release point, under steady-state conditions, during ebb tide	24
8	Observed dye distribution and predicted distribution of excess temperature at section 6000 yd downstream from release point, under steady-state conditions, during ebb tide	25
9	Observed dye distribution and predicted distribution of excess temperature at section 8000 yd downstream from release point, under steady-state conditions, during ebb tide	26

ILLUSTRATIONS (cont.)

Figure — Page

10 Observed dye distribution and predicted distribution of excess temperature at section 1000 yd upstream from release point, under steady-state conditions, during flood tide 27

11 Observed dye distribution and predicted distribution of excess temperature at section 2000 yd upstream from release point, under steady-state conditions, during flood tide 28

12 Observed dye distribution and predicted distribution of excess temperature at section 3000 yd upstream from release point, under steady-state conditions, during flood tide 29

13 Observed dye distribution and predicted distribution of excess temperature at section 4000 yd upstream from release point, under steady-state conditions, during flood tide 30

14 Observed dye distribution and predicted distribution of excess temperature at section 6000 yd upstream from release point, under steady-state conditions, during flood tide 31

15 Observed dye distribution and predicted distribution of excess temperature at section 8000 yd upstream from release point, under steady-state conditions, during flood tide 32

16 Horizontal distribution of predicted excess temperature downstream from heat source on ebb tide for an assumed heated layer thickness $D_h = 4$ ft 33

17 Horizontal distribution of predicted excess temperature upstream from heat source on flood tide for an assumed heated layer thickness $D_h = 4$ ft 34

Introduction

This paper treats the problem of predicting the probable distribution of excess temperature resulting from the discharge of a heated effluent into a tidal estuary. Here excess temperature means the difference between the temperature which would prevail under conditions of a heated discharge and the temperature which would prevail under "natural" conditions. It is believed that the techniques described here will have general application; however, this paper treats the specific case of the heated effluent from the PEPCO Chalk Point Power Plant on the Patuxent estuary in Maryland, which should serve to illustrate the basic concepts.

The PEPCO Chalk Point Power Plant is a conventional plant using fossil fuel. The procedure described here may be of considerable value in assessing the environmental effects of a nuclear power plant located on an estuarine body of water, since, with existing technology, the required heat dissipation per kilowatt of produced power is significantly greater for a nuclear-powered electric plant than for modern, highly efficient conventional electric plants. In several nuclear plants now under consideration it appears that the heated discharge may be of more concern from the standpoint of possible environmental effects than the release of low-level radioactivity.

Fig. 1 shows the Patuxent tidal estuary in the vicinity of Chalk Point. A power plant is being placed into operation at Chalk Point. It is the plan ultimately to install four 350 MW generators at this site. Initially, however, the plant is to go into operation with a single 350 MW unit, and it is for this initial condition that our computations are made.

Cooling water for the condensers is to be drawn from the south side of Chalk Point near the entrance to Swanson Creek. After passing through the condenser, the cooling water flows through a canal constructed parallel to the estuary and extending northward for a distance of approximately 7,000 ft. A pair of jetties extending a short distance into the estuary directs the discharge into the waterway at a point approximately opposite Potts Point. The canal is approximately 10 ft deep and 100 ft wide. The insert in Fig. 1 shows somewhat schematically the general features of the intake-outlet arrangement in respect to the adjacent estuary. A diked-in landfill has been built out into the estuary adjacent to the plant site in an attempt to deflect warm discharge water from the intake structure.

Our approach to the problem of prediction of the probable excess temperature distribution resulting from the heated discharge involves 1) evaluation of the physical processes of movement and dispersion of the effluent in the estuary through the use of a tracer fluorescent dye to simulate the effluent, and 2) correction of the conservative distribution obtained from the tracer experiments for the nonconservative processes of boundary cooling. The next section of this report describes the dye tracer experiments, following which is a

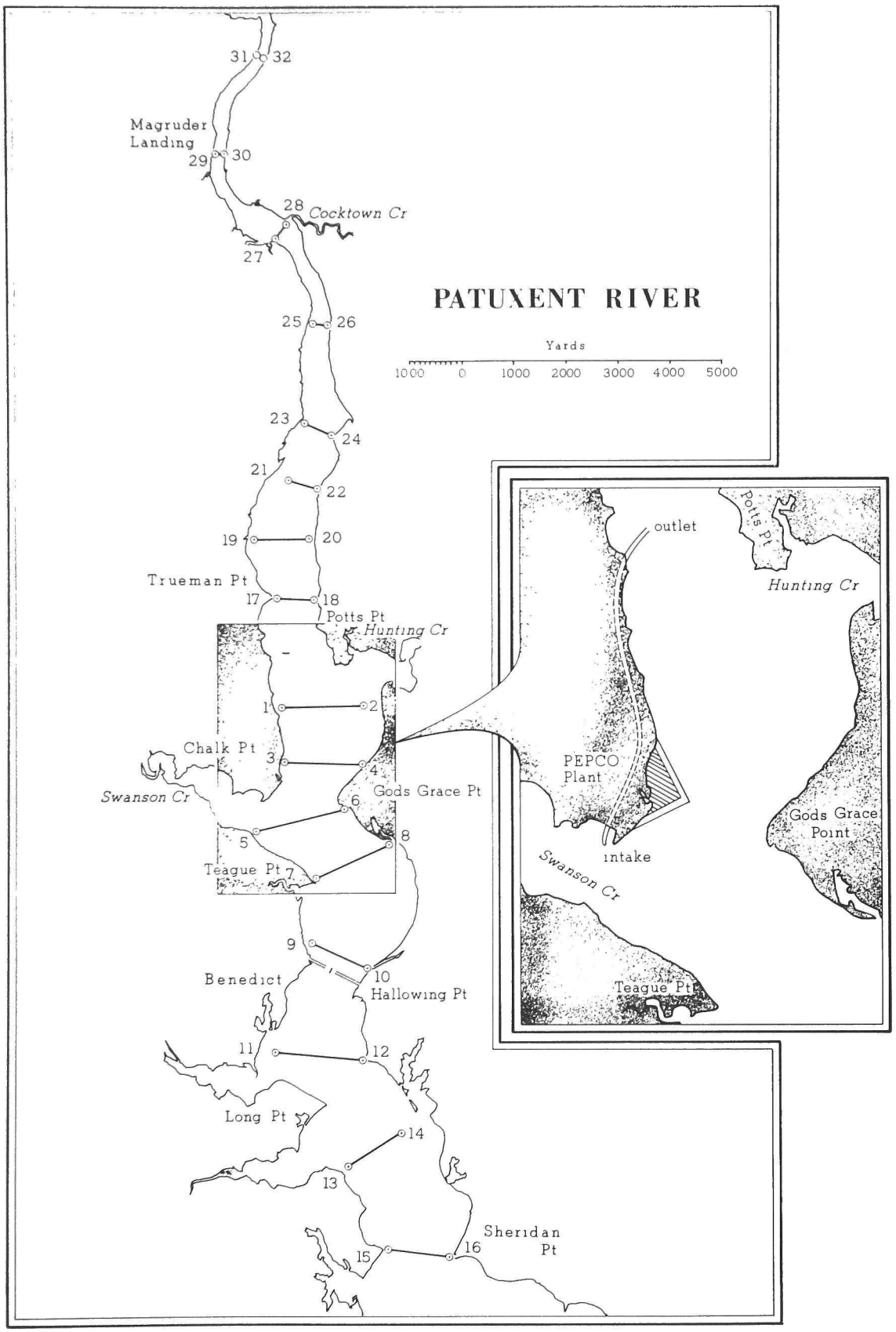

Fig. 1. Patuxent River estuary showing location of upstream and downstream cross sections. Insert shows immediate vicinity of ~~PEPCO plant~~ with location of intake and outlet for cooling water.

presentation of the theoretical basis for the correction of the observed distribution of tracer dye to take into account the nonconservative processes of heat loss at the surface.

Field Study of Dispersion

The use of rhodamine dyes to study the processes of movement and turbulent diffusion in an estuary has been discussed by Pritchard and Carpenter (1960)*. In the present case, it was not possible for us to introduce the tracer dye in the same manner that the excess heat will be introduced into the estuary, in that the volume rate of flow of the dye solution is very small compared to the volume rate of flow of the actual heated effluent. Both theory and experience show that the volume rate of discharge of a contaminant is important only close to the point of discharge. For distances further removed from the discharge point the distribution of contaminant concentration will be independent of the volume in which the contaminant was distributed prior to discharge.

In order to minimize the distance over which the distribution of dye concentration is not representative of the probable distribution of excess heat, the dye was introduced in a manner designed to provide for initial mechanical mixing over a line source in the estuary having a length approximately equal to the initial width of the effluent plume at discharge. Six poles were driven into the bottom at 20-ft intervals

---

* Pritchard, D.W. and J.H. Carpenter (1960) Measurements of turbulent diffusion in estuarine and inshore waters: Bull. Internat. Assoc. Sci. Hydrol. No. 20, 37-50.

along a line running from the western edge of the channel toward the western shore, at a point approximately opposite the proposed terminus of the canal from which the heated effluent will be discharged. Vertical diffusers designed to discharge dye solution uniformly over the depth from surface to bottom were mounted on each pole, and polyethylene hoses were run from the poles to a nearby anchored vessel. A 40% rhodamine B dye solution, made up to have a specific gravity of 1.03, was metered into a flow of 18 gal min^{-1} which was pumped from the estuary waters alongside the vessel. This initial dilution of 1:2800 of the dye solution provided for effective elimination of the slight density difference between the raw dye solution and the receiving waters. The mechanical dispersion afforded by the vertical diffusers further provided for initial complete vertical mixing of the introduced tracer.

The discharge from the pump, after mixing with the introduced dye, was divided into six equal effluent streams by use of a series of valved T-fittings. The flow in each of the six discharge lines was monitored by use of rotometer flow indicators and maintained at constant equal values by appropriate valve adjustments.

The dyed discharge from each of the six diffusers was observed to extend down-current as a plume. These individual plumes soon began to merge, and at 1000 yd from the discharge the observed profile of dye concentration across the estuary did not show any consistent features attributable to the multi-source origin of the discharge. That is, at 1000 yd the discharge appeared to be an evenly distributed line source.

The dye was released at a rate of 10 pounds of dry dye per day for a ten-day period from the 2nd through the 11th of October, 1963. The dye concentration was measured at cross sections located at 1000, 2000, 3000, 4000, 6000, 8000, 10,000, and 12,000 yd upstream and downstream from the discharge point. The locations of these sections are shown on Fig. 1. The downstream sections were occupied during ebb tide and the upstream sections during flood tide. Data obtained at the 10,000 and 12,000 yd sections were insufficient to utilize in the evaluation below, although they did indicate that the temperature increase due to the heated discharge would be quite small at points that far removed from the outfall.

Theoretical Considerations

The methods developed here for the forecast of temperature distribution are based upon the following concepts:

1) The effects of the physical processes of movement and dispersion of the added heat from a given parcel of the effluent may be linearly combined with the heat loss across the surface of the parcel due to radiation, evaporation, and conduction, to give the net overall horizontal distribution of heat.

2) The observed horizontal distribution of the tracer fluorescent dye, taking into account the appropriate factors for discharge rate and depth of vertical spread, may be used to determine the probable distribution of heat under conditions of no boundary heat loss.

3) The incremental increase in heat flux across the surface boundary due to radiation, evaporation, and conduction may be approximated as

a linear function of the difference between the temperature under conditions of the heated discharge and the temperature under "natural" conditions.

Item 2) in the previous paragraph leads to the relationships

$$(1) \quad \frac{\Gamma_{h,o}(t)}{Q_h} \cdot D_h = \frac{\Gamma_d(t)}{Q_d} \cdot D_d$$

and

$$(2) \quad \frac{\Gamma_{h,o,\infty}}{Q_h} \cdot D_h = \frac{\Gamma_{d,\infty}}{Q_d} \cdot D_d$$

where:

$\Gamma_{h,o}(t)$ = concentration of excess heat at a given point in the estuary at a time t after initiation of a continuous discharge, under conditions of no loss of heat by cooling

$\Gamma_{h,o,\infty}$ = steady state concentration of excess heat at a given point in the estuary resulting from a continuous discharge for an infinite time, under conditions of no heat loss by cooling

$\Gamma_d(t)$ = concentration of dye at a given point in the estuary at a time t after initiation of a continuous discharge

$\Gamma_{d,\infty}$ = steady state concentration of dye at a given point in the estuary resulting from a continuous discharge for an infinite time

Q_d = rate of discharge of dye

Q_h = rate of discharge of heat

D_d = vertical extent of dye distribution

D_h = vertical extent of excess heat distribution.

Now, if we further designate:

$\Gamma_h(t)$ = concentration of heat at a given point in the estuary at a time t after initiation of a continuous discharge, taking into account heat loss by cooling

$\Gamma_{h,\infty}$ = steady state concentration of heat at a given point in the estuary resulting from a continuous discharge for an infinite time, taking into account heat loss by cooling

then we may write:

$$(3) \quad \Gamma_{h,\infty} = \int_0^\infty \frac{\partial \Gamma_h(t)}{\partial t}\, dt$$

Under the assumption that the excess heat flux across the surface resulting from evaporation, radiation, and conduction can be approximated by a linear function of the excess temperature (i.e., temperature under conditions of heated discharge minus the temperature under "natural" conditions), it is shown in the appendix to this paper that

$$(4) \quad \frac{\partial}{\partial t}\left\{\Gamma_h(t)\right\} = \frac{\partial}{\partial t}\left\{\Gamma_{h,o}(t)\right\} \cdot e^{-\gamma t/D_h}$$

where γ is a rate coefficient, the value of which depends on wind velocity, temperature of the heated effluent, and the "natural", or unheated, temperature of the receiving waters. For normal summertime conditions γ is equal to approximately 0.1 ($\pm$0.05) ft hr^{-1}.

From equation (1),

$$(5)\quad \Gamma_{h,o}(t) = \frac{Q_h}{Q_d} \cdot \frac{D_d}{D_h} \cdot \Gamma_d(t)$$

and substituting equations (4) and (5) into (3) gives

$$(6)\quad \Gamma_{h,\infty} = \int_0^\infty \frac{\partial}{\partial t}\left\{\Gamma_{h,o}(t)\right\} \cdot e^{-\gamma t/D_h} \cdot dt$$

$$= \frac{Q_h}{Q_d} \cdot \frac{D_d}{D_h} \int_0^\infty \frac{\partial}{\partial t}\left\{\Gamma_d(t)\right\} \cdot e^{-\gamma t/D_h} \cdot dt$$

The dye concentration at a given point in the estuary will of course vary over the tidal cycle, reaching maximum values at points downstream from the discharge point at or soon after the time of peak ebb flow, and reaching maximum values at points upstream from the discharge point at or soon after the time of peak flood. In Fig. 2 the peak concentration observed across the section 3000 yd downstream from the discharge point is plotted as a function of time during ebb tide, on the 15th tidal period after initiation of release. During the first portion of the ebb period relatively constant low concentrations are observed. Just after maximum ebb flow the concentration begins to increase rapidly, reaching a maximum value about one hour after peak ebb flow. This first maximum is associated with the arrival of the pool of dye which accumulates around the discharge point during the period of slack water. The relative intensity of this first maximum should be reduced under conditions of the large volume rate of effluent discharge characteristic of actual plant operation. After this maximum, the concentration decreases slightly with time, and then rises to a relatively flat second maximum. This short plateau in the concentration time plot over a tidal cycle represents, to a first approximation,

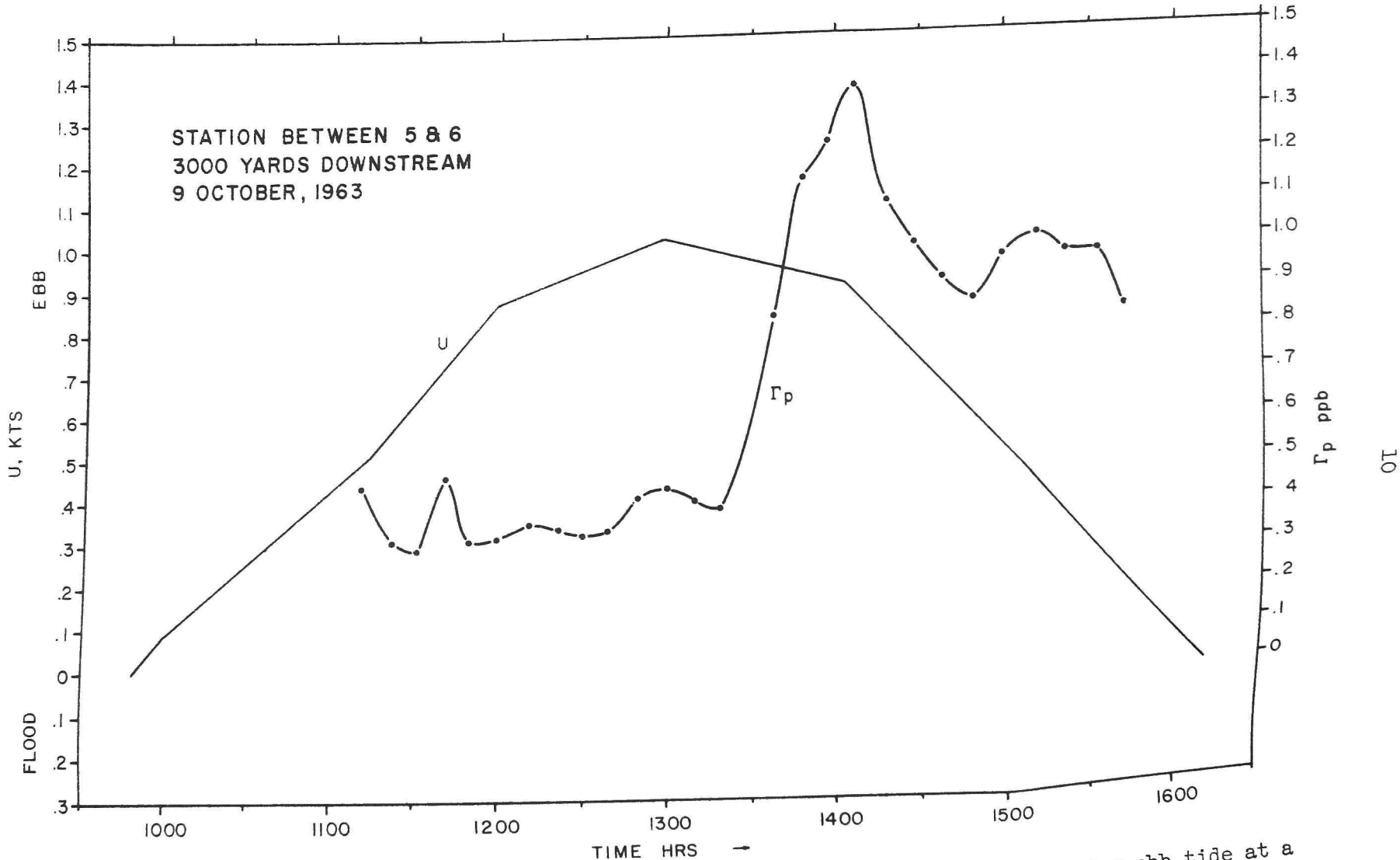

Fig. 2. Ebb current U (kt) and peak dye concentration Γ_p (ppb) as a function of time during ebb tide at a section 3000 yd downstream from the discharge point, on the 15th tidal cycle after initiation of dye discharge.

the concentration which would have occurred had the flow been constant in the ebb direction over the period of discharge, rather than oscillating with tidal period.

In the following treatment we will be concerned with the concentration at this second maximum in the concentration-time plot over a tidal cycle, since we consider that this concentration is more representative of the conditions which will prevail for the actual heated discharge than is the first, somewhat higher maximum. As pointed out above, the first maximum is associated with a pool of tracer which accumulates around the discharge at slack water. If the tracer dye had been discharged in a volume rate of flow equal to that which will prevail under actual plant operations, the flow produced by such a discharge would lead to a smoothing out of the first maximum so that it would merge with the second maximum producing a period of about two hours during each tidal cycle when a relatively flat plateau of maximum concentrations would occur.

The concentration at the time of the second maximum is designated as the characteristic tracer concentration. On the basis of repeated sampling over portions of a tidal cycle, the time of the characteristic concentration relative to the time of maximum current was determined for each section. During the course of the experiment repeated crossings of each section upstream and downstream from the release point were made for a period of approximately one hour about the time of the characteristic concentration. The individual records of dye concentration versus distance across the section generally showed a maximum value at some point in the section with decreasing concentra-

tions toward each shore. The position of the maximum and the concentration at the maximum varied slightly as the larger-scale eddies in the flow pattern caused the plume of tracer to meander; however, the maximum was almost always found in the same general area of the cross-section. The records from the several crossings of section near the time of the characteristic concentration were averaged in the following way: (a) the average position of the peak concentration in the section was found, and each curve of dye concentration vs. distance across the section was displaced so that all peaks coincided at this average position; (b) the displaced curves were then averaged to produce a smoothed curve of concentration vs. distance across the section. This method of smoothing retains the characteristic shape of the concentration distribution across the section while removing transient irregularities of short time period.

When the characteristic concentration thus determined for each section, for each day during the period of discharge, is plotted against time, the characteristic concentration is seen to approach a nearly constant value, representing the steady state concentration, in approximate accordance to an exponential relationship. Fig. 3 shows such a plot for data observed at the section 4000 yd downstream from the discharge point. Thus $\Gamma_d(t)$ approaches $\Gamma_{d,\infty}$ asymptotically with time according to the relationship

$$(7) \qquad \Gamma_d(t) = \Gamma_{d,\infty} (1 - e^{-\eta t})$$

where η is a rate constant which is determined by the best fit of the data for each section. It is noted that for the data plotted in Fig. 2,

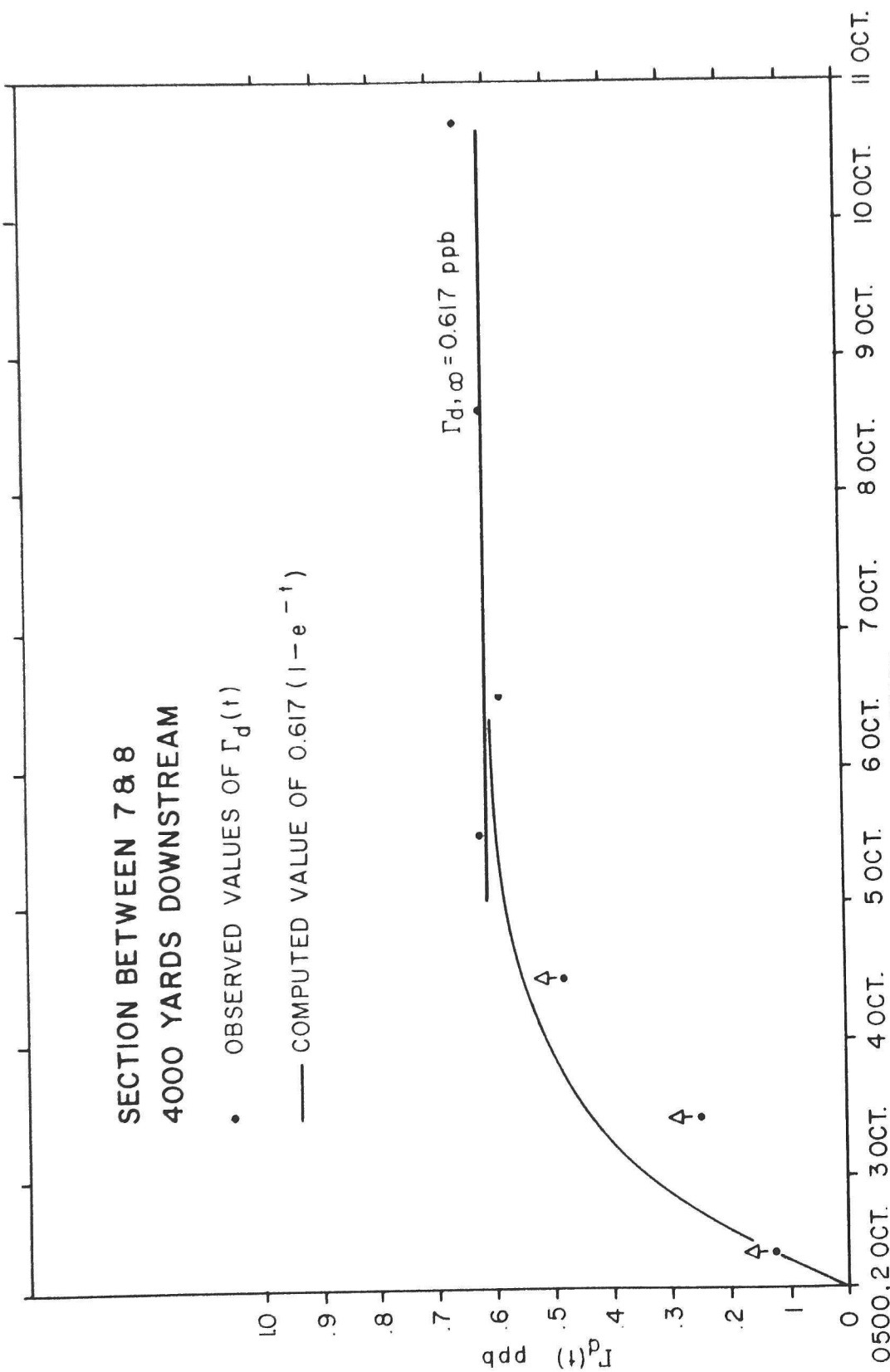

Fig. 3. Characteristic concentration $\Gamma_d(t)$ as a function of time over the duration of the experiment at a section 4000 yd downstream from release point.

$\eta \doteq 1.0\ \text{day}^{-1}$, and this value was found to be fairly representative for all sections. From equation (7), we have

$$(8) \quad \frac{\partial}{\partial t}\left\{ \Gamma_d(t) \right\} = \Gamma_{d,\infty} \cdot \eta \cdot e^{-\eta t}$$

which, when substituted in equation (6), gives

$$(9) \quad \Gamma_{h,\infty} = \frac{Q_h}{Q_d} \cdot \frac{D_d}{D_h} \int_0^\infty \Gamma_{d,\infty}\, \eta e^{-\eta t} \cdot e^{-\gamma t/D_h} \cdot dt$$

The integration can now be carried out to give

$$(10) \quad \Gamma_{h,\infty} = \frac{Q_h}{Q_d} \cdot \Gamma_{d,\infty} \left\{ \frac{D_d}{D_h + \gamma/\eta} \right\}$$

Equation (10) allows us to compute the probable distribution of heat ($\Gamma_{h,\infty}$) from the observed distribution of dye ($\Gamma_{d,\infty}$). The rate of discharge of heat, Q_h, is equal to the rate of heat dissipation at the condensers, since the heat loss during transit of the canal is relatively unimportant. To see that this is so, consider equation (A-11) given in the appendix:

$$\theta_\tau = \theta_o e^{-\gamma\tau/D}$$

where θ_o is the initial excess temperature of a volume of heated water; θ_τ is the excess temperature after time τ; D is the depth over which the excess heat is distributed; and γ is a rate coefficient equal to approximately 0.1 ft hr^{-1} for normal summer conditions. Under conditions of maximum discharge, the flow rate in the canal will be about 1 ft sec^{-1}, and hence a parcel of water passing from the condensers would take about 2 hr to travel along the 7000-ft length of the canal. The depth of the canal is about 10 ft. Using the values in the above equation we have

$$\theta_\tau = \theta_o \, e^{-0.1(2/10)} = \theta_o \, e^{-0.02} = 0.98 \, \theta_o$$

Thus the excess temperature at discharge from the end of the canal will still be 98% of the excess temperature at the condensers.

According to information supplied by PEPCO, the heat dissipation at the condensers will be approximately 4.3×10^6 BTU per hr per megawatt of produced power, or for the first unit of 350 MW, $Q_h = 1.5 \times 10^9$ BTU $hr^{-1} = 36 \times 10^9$ BTU day^{-1}.

The rate of discharge of dye in this experiment was 10 pounds day^{-1}. The concentration of dye, $\Gamma_{d,\infty}$, is given in ppb, i.e., in 10^{-9} pounds $pound^{-1}$. Now, one BTU is the amount of heat required to raise the temperature of one pound of water 1 degree F. Therefore, if we express the concentration of excess heat, $\Gamma_{h,\infty}$, in BTU $pound^{-1}$, we have directly the excess temperature in degrees F. Thus

$$\Gamma_{h,\infty} = \theta = \frac{36 \times 10^9}{10} \cdot 10^{-9} \, \Gamma_{d,\infty} \left\{ \frac{D_d}{D_h + \gamma/\eta} \right\}$$

or

$$\theta = 3.6 \cdot \Gamma_{d,\infty} \left\{ \frac{D_d}{D_h + \gamma/\eta} \right\} \tag{11}$$

where θ is the excess temperature in degrees F and $\Gamma_{d,\infty}$ is the dye concentration expressed in ppb.

Computation of the Probable Distribution of Excess Temperature

The data available for the computation of the probable distribution of excess temperature from the heated discharge from the Chalk Point plant consist of repeated records of the dye concentration across sections located at distances of 1000, 2000, 3000, 4000, 6000, and 8000 yd upstream and downstream from the discharge point. Except for runs taken for the purpose of establishing the features of the time variation in concentration during a tidal cycle, which in turn provided information as to the time of the characteristic concentration relative to the time of slack water before the flood or ebb current, most of the records of dye concentration across a given section were made over a short time period about the time of the characteristic concentration. This time occurred during the flood tide for sections upstream from the discharge point, and during the ebb tide for sections downstream from the discharge point. In general, the interval between the times of current reversal and the time of the characteristic concentration increased with distance from the discharge point.

For each section, the characteristic concentration was plotted against time as described earlier and as illustrated by Fig. 3. The plotted data were compared to the relationship

$$\Gamma_d(t) = \Gamma_{d,\infty} (1 - e^{-\eta t})$$

and a best-fit value of η determined. For all sections it was found that a value of $\eta = 1.0$ day $^{-1}$ gave reasonable fits to the observed data.

As described earlier, smoothed curves of the dye distribution

across each section were determined from the several repeated crossings made near the time of the characteristic concentration for each day of the experiment for which sufficient data were available. The dye was discharged for the ten-day period 2 October through 11 October, 1963. The plots of time vs. characteristic concentration indicated that steady state conditions were reached at each section by the 5th or 6th of October. Data collected after the 6th of October then served for the determination of $\Gamma_{d,\infty}$ across each section, for use in equation (11).

As shown in the appendix, a reasonable value for γ under summertime conditions is 0.1 ft hr^{-1} or 2.4 ft day^{-1}. The ratio of γ to η in equation (11) is then

$$\gamma/\eta = \frac{2.4 \text{ ft day}^{-1}}{1.0 \text{ day}^{-1}} = 2.4 \text{ ft}$$

The dye was introduced uniformly from surface to bottom from six diffusers evenly spaced along a line 100 ft in length extending from the western edge of the channel toward the west shore of the Patuxent. As the dye spread over deeper water, the vertical mixing produced nearly uniform concentrations in the vertical. We have therefore taken the depth over which the dye was distributed, D_d, to be the mean volume depth of the estuary. Though there was some variation in mean depth from section to section, we have taken a constant value of 8.4 ft for the 8000 yd downstream from the discharge point, and another constant value of 9.7 ft for the 8000 yd upstream from the discharge point.

The one most uncertain parameter in equation (11) is the depth over which the heat will be distributed. This heated layer may be as shallow as 2 ft in some instances and as deep as the mean depth of the

estuary in other instances. We have chosen to evaluate equation (11) for the three selected D_h values of 4 ft, 6 ft, and 8 ft. Putting these various values in equation (11), we find:

(12) (a) $\theta F = 4.73\ \Gamma_{d,\infty}$ for $D_h = 4$ ft, downstream

(b) $\theta F = 3.60\ \Gamma_{d,\infty}$ for $D_h = 6$ ft, downstream

(c) $\theta F = 2.91\ \Gamma_{d,\infty}$ for $D_h = 8$ ft, downstream

(d) $\theta F = 5.47\ \Gamma_{d,\infty}$ for $D_h = 4$ ft, upstream

(e) $\theta F = 4.15\ \Gamma_{d,\infty}$ for $D_h = 6$ ft, upstream

(f) $\theta F = 3.38\ \Gamma_{d,\infty}$ for $D_h = 8$ ft, upstream

It is probable that D_h will in fact increase with distance from the source. On the other hand, though our data were insufficient to reveal the trend, the rate constant η is also likely to increase with distance from the source, and like changes in these two parameters as they occur in equation (11) are somewhat compensating. Considering the possible ranges in the various parameters in equation (11), we have confidence in our computations to about ±30%.

Figs. 4 through 9 show the results of our computations for the sections downstream from the release point, and Figs. 10 through 15 show the results for sections upstream from the release point. In each of these figures the bottom profile across the section is shown in the upper part of the diagram. In the lower part of the diagram four curves are shown in each figure. One of the curves gives the concentration of dye as a function of distance across the section, with the scale in ppb entered on the left-hand vertical axis. The three other curves give the computed excess temperature for the three assumed values of D_h, that is, for D_h equal to 4 ft, 6 ft, and 8 ft.

The excess temperature scale in degrees F is entered on the right-hand vertical axis.

The excess temperature values computed for each section for the case of $D_h = 4$ ft were plotted on a horizontal chart of the estuary and contours of equal excess temperature drawn. Fig. 16 shows the horizontal distribution of the predicted excess temperature which we expect will occur downstream from the discharge point, and Fig. 17 is the corresponding distribution for the area upstream from the discharge. Fig. 16 applies to a period of approximately two hours' duration after the time of maximum ebb current, and Fig. 17 applies to a period of approximately two hours' duration after maximum flood current. These excess temperature distributions are computed for the case of a single 350 MW unit. To a first approximation, the excess temperature is directly proportional to the heat dissipated at the condensers, and hence to the total production of power. Therefore, in order to predict the probable excess temperature for the future installation of additional 350 MW units, the values given here should be multiplied by the number of such units on the line.

No attempt has been made to extend our predictions into the area within 1000 yd from the discharge. Within this area the relatively large volume rate of discharge which will occur in the case of the actual plant effluent will probably influence the distribution of contaminant. Beyond 1000 yd or so, we consider that the only characteristic of the source which remains important is the source strength, that is, the amount of contaminant introduced per unit time (i.e., pounds of dye day^{-1}, or BTU day^{-1}). There is in fact ample evidence

from other studies that the initial volume containing the introduced contaminant is not an important factor in determining the concentration distribution at distances sufficiently far removed from the discharge point.

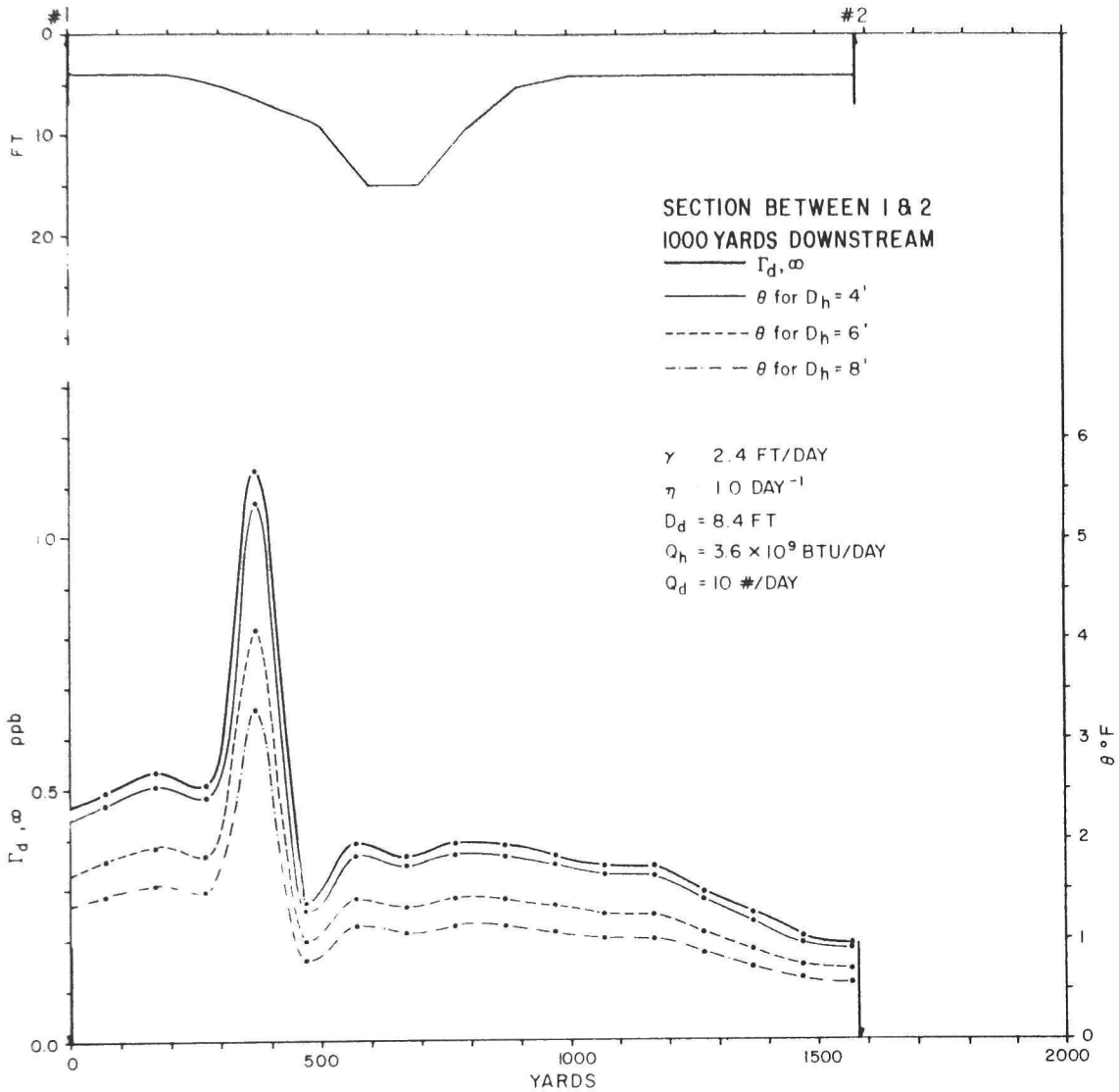

Fig. 4. Observed dye distribution and predicted distribution of excess temperature at section 1000 yd downstream from release point, under steady-state conditions, during ebb tide.

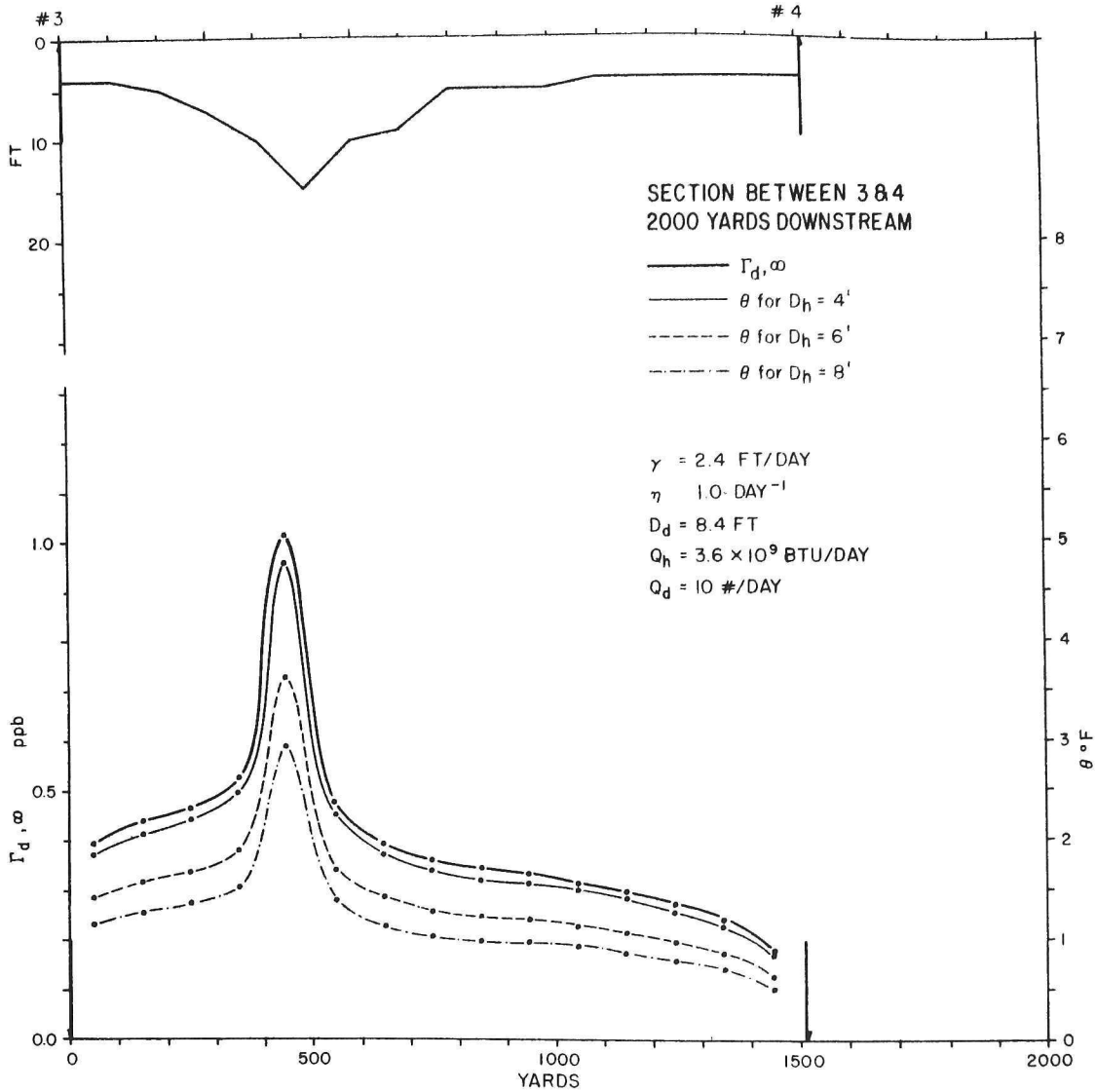

Fig. 5. Observed dye distribution and predicted distribution of excess temperature at section 2000 yd downstream from release point, under steady-state conditions, during ebb tide.

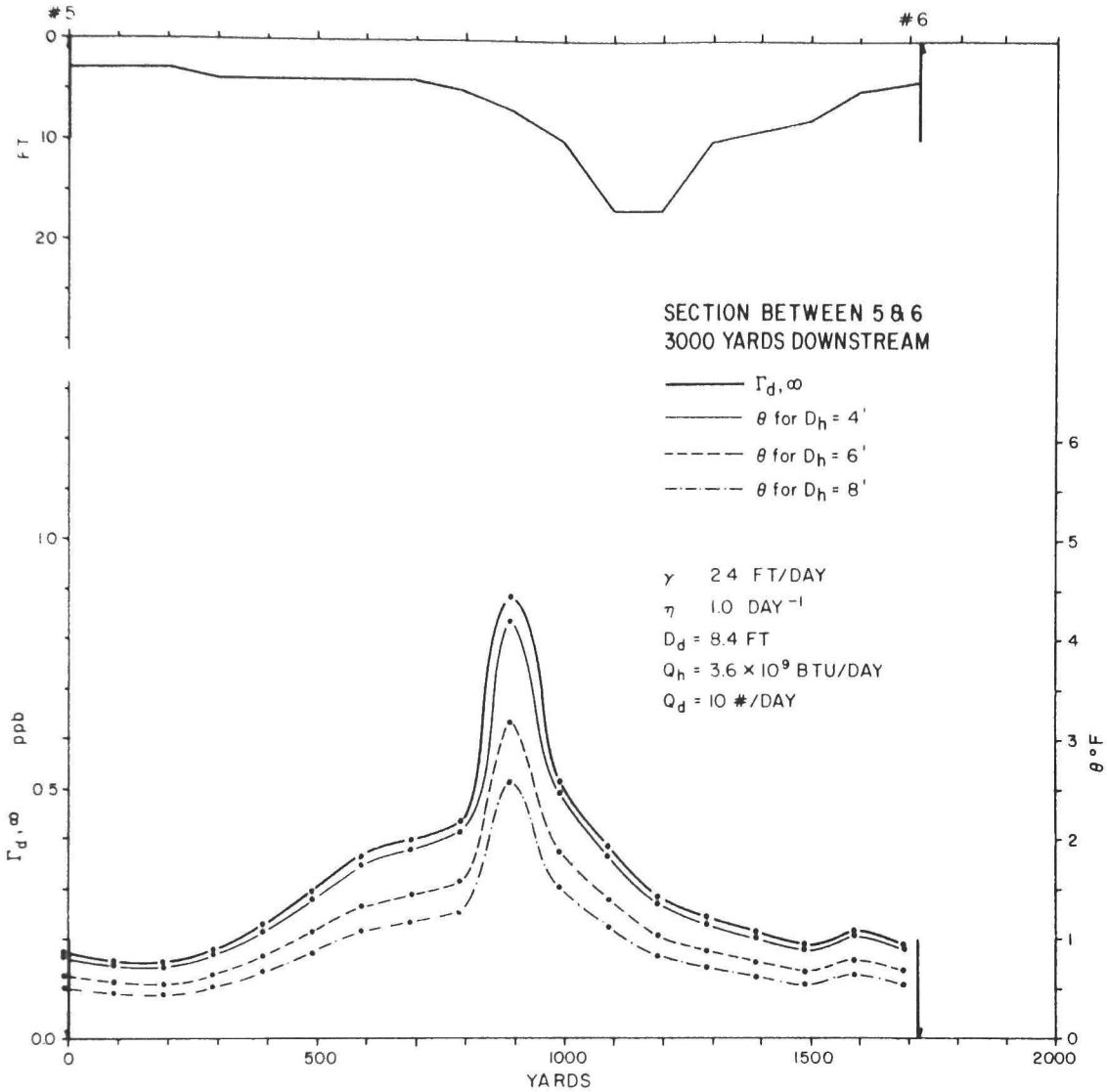

Fig. 6. Observed dye distribution and predicted distribution of excess temperature at section 3000 yd downstream from release point, under steady-state conditions, during ebb tide.

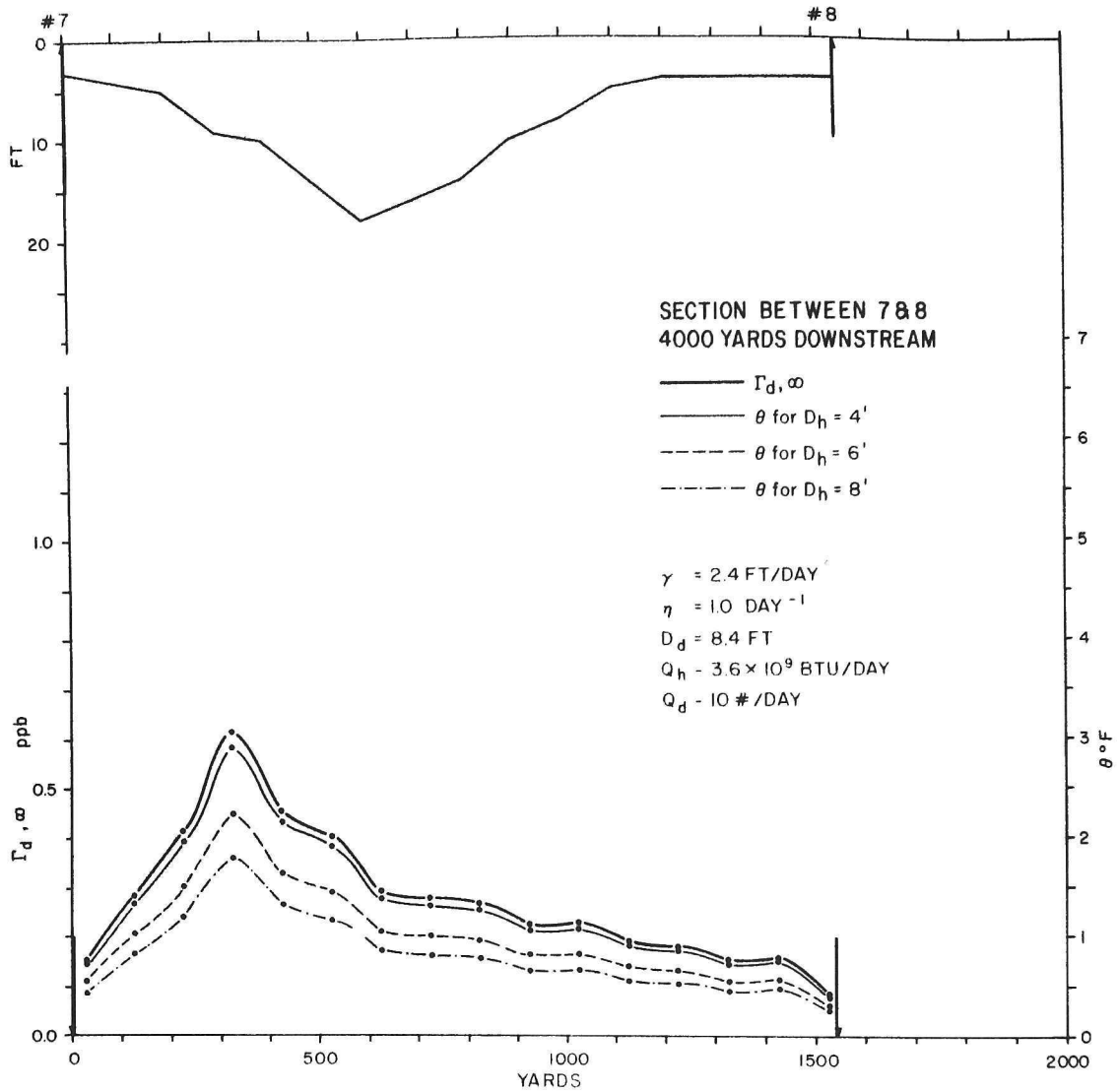

Fig. 7. Observed dye distribution and predicted distribution of excess temperature at section 4000 yd downstream from release point, under steady-state conditions, during ebb tide.

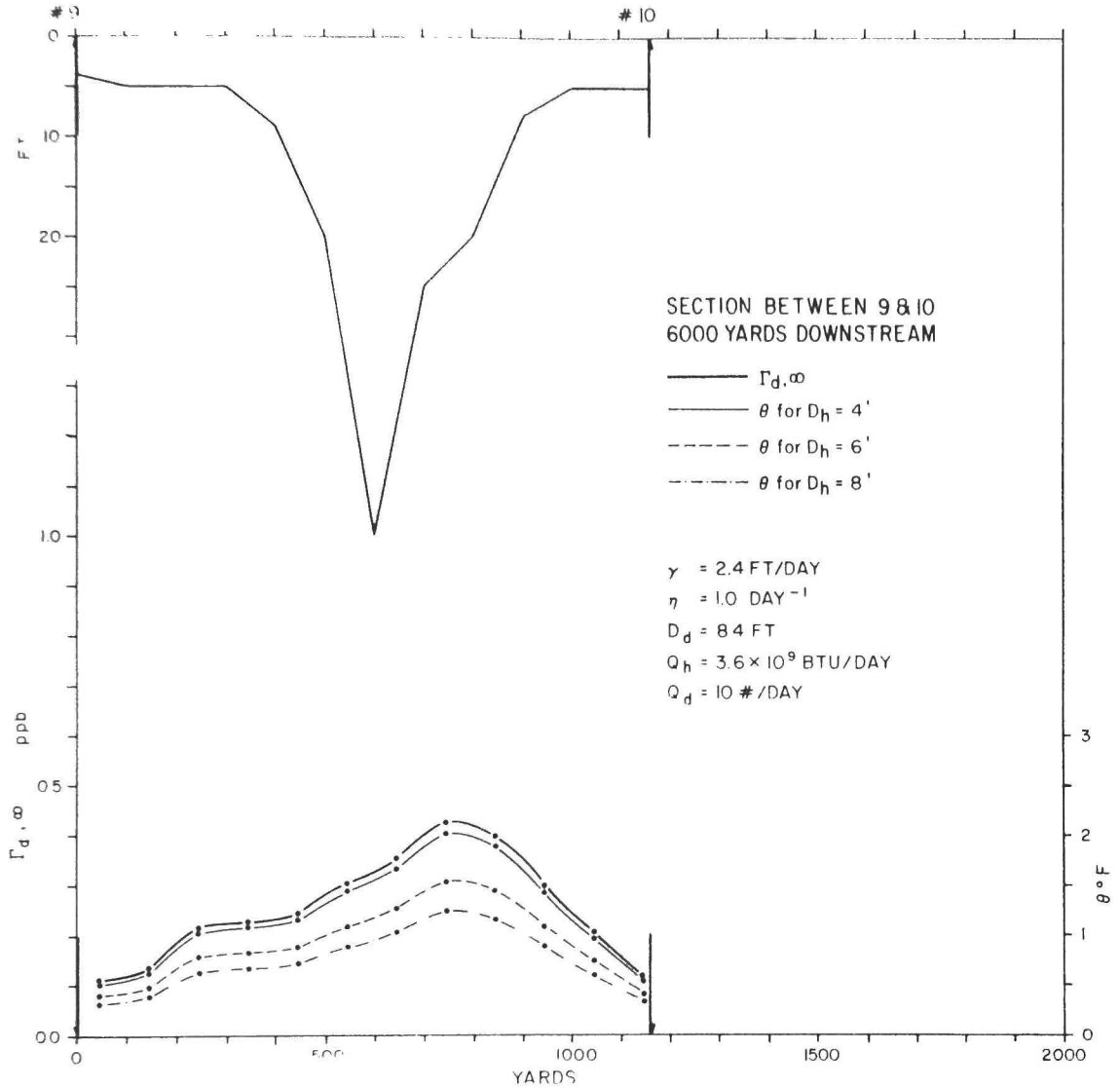

Fig. 8. Observed dye distribution and predicted distribution of excess temperature at section 6000 yd downstream from release point, under steady-state conditions, during ebb tide.

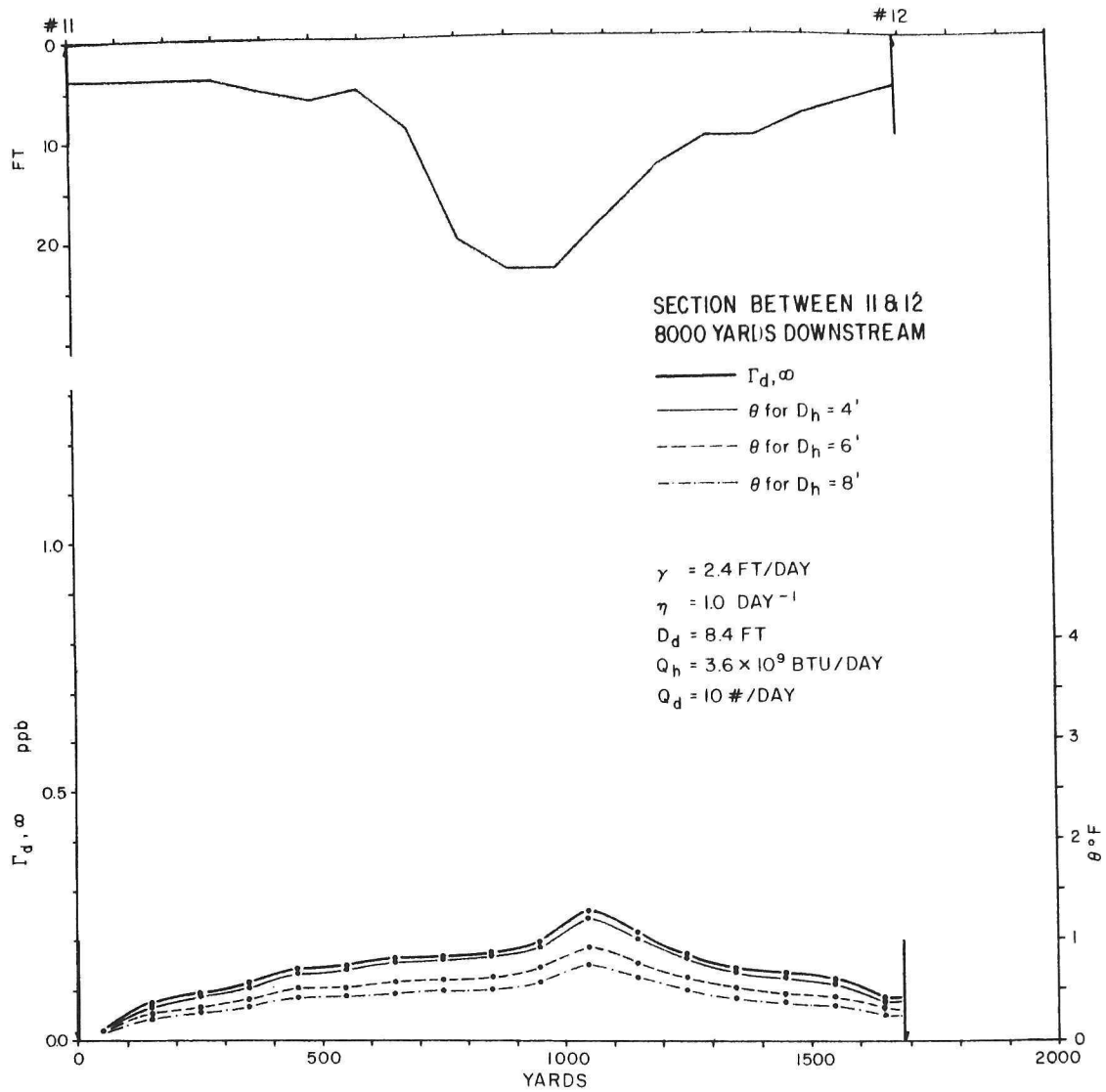

Fig. 9. Observed dye distribution and predicted distribution of excess temperature at section 8000 yd downstream from release point, under steady-state conditions, during ebb tide.

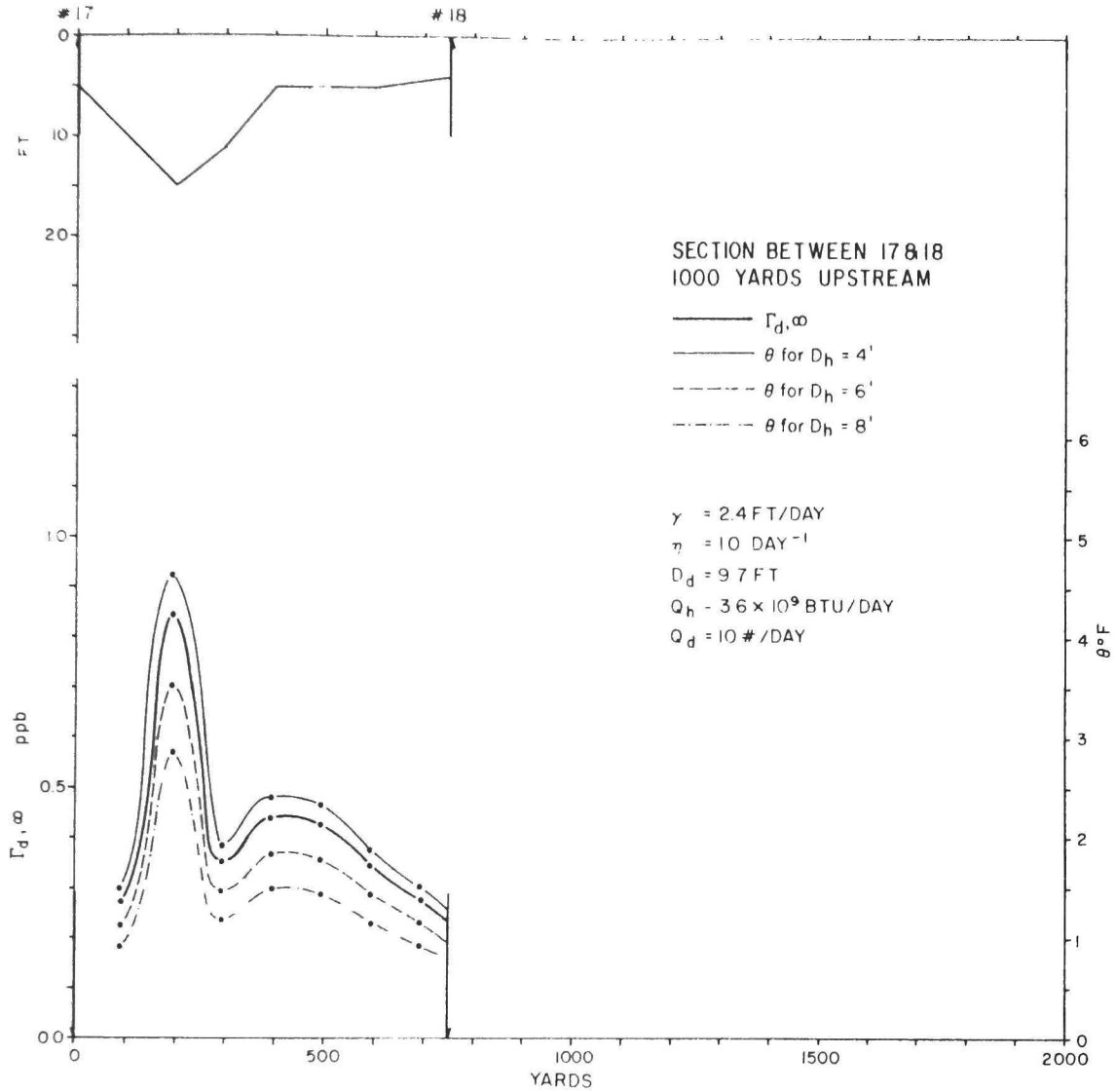

Fig. 10. Observed dye distribution and predicted distribution of excess temperature at section 1000 yd upstream from release point, under steady-state conditions, during flood tide.

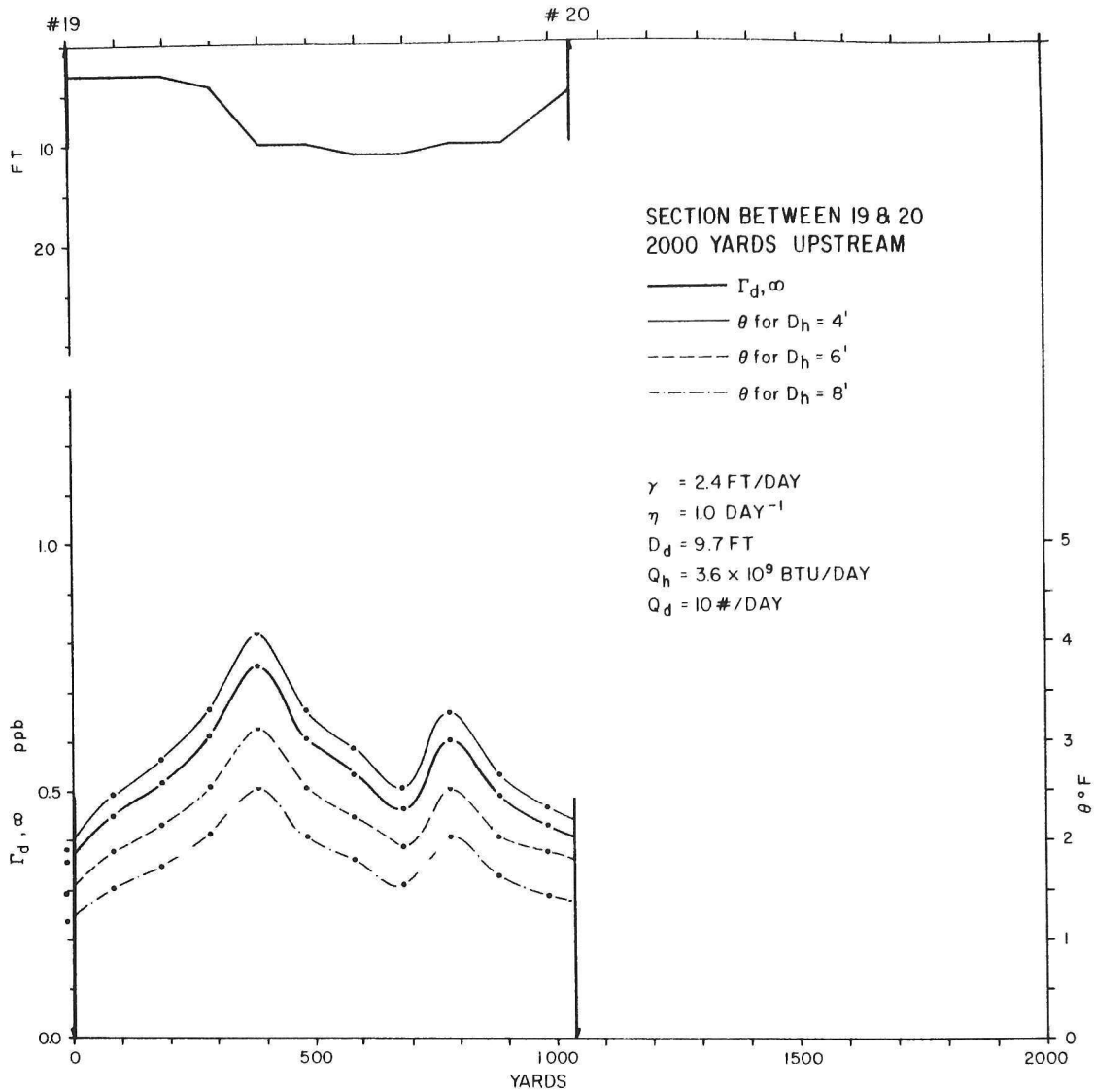

Fig. 11. Observed dye distribution and predicted distribution of excess temperature at section 2000 yd upstream from release point, under steady-state conditions, during flood tide.

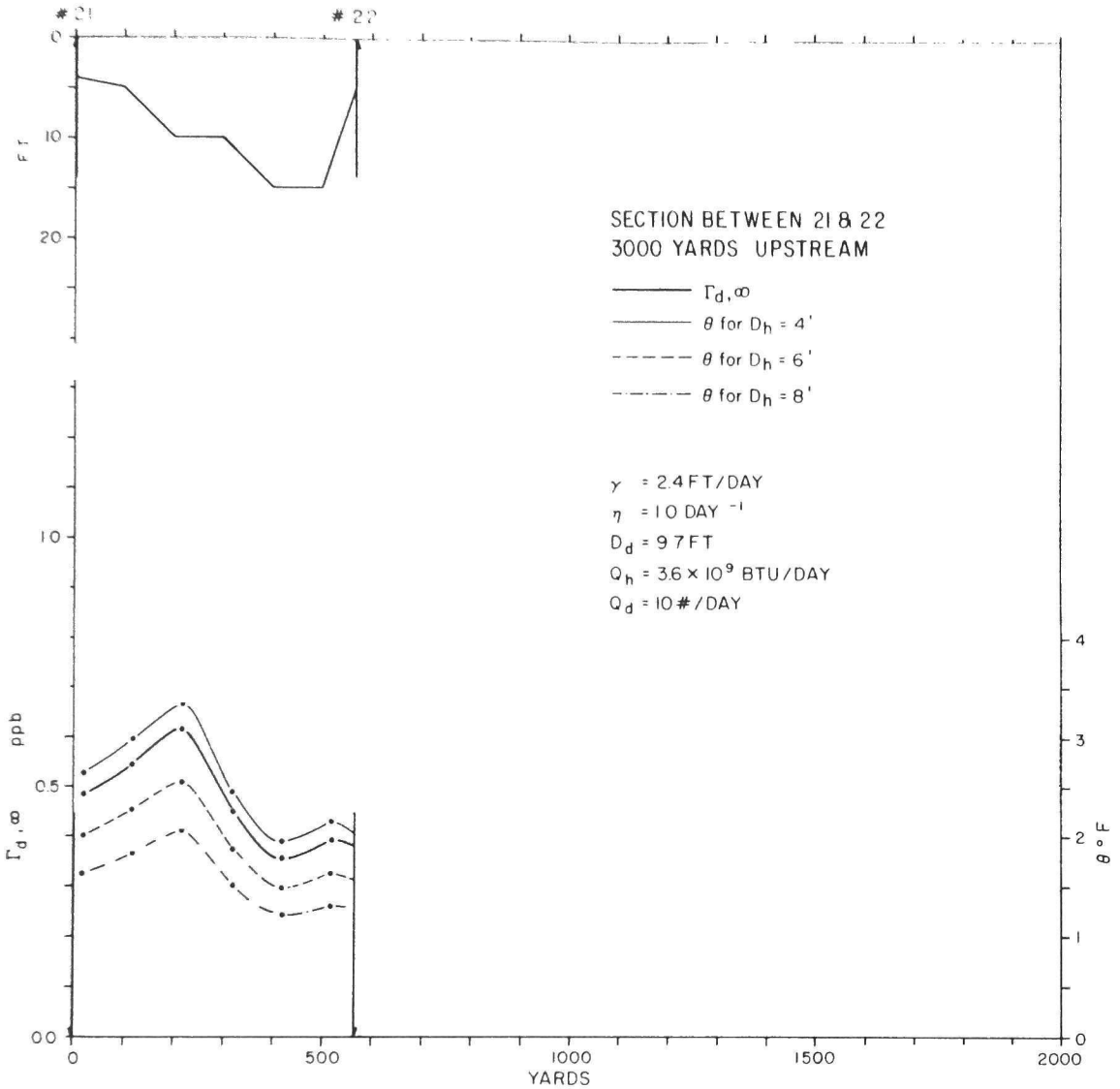

Fig. 12. Observed dye distribution and predicted distribution of excess temperature at section 3000 yd upstream from release point, under steady-state conditions, during flood tide.

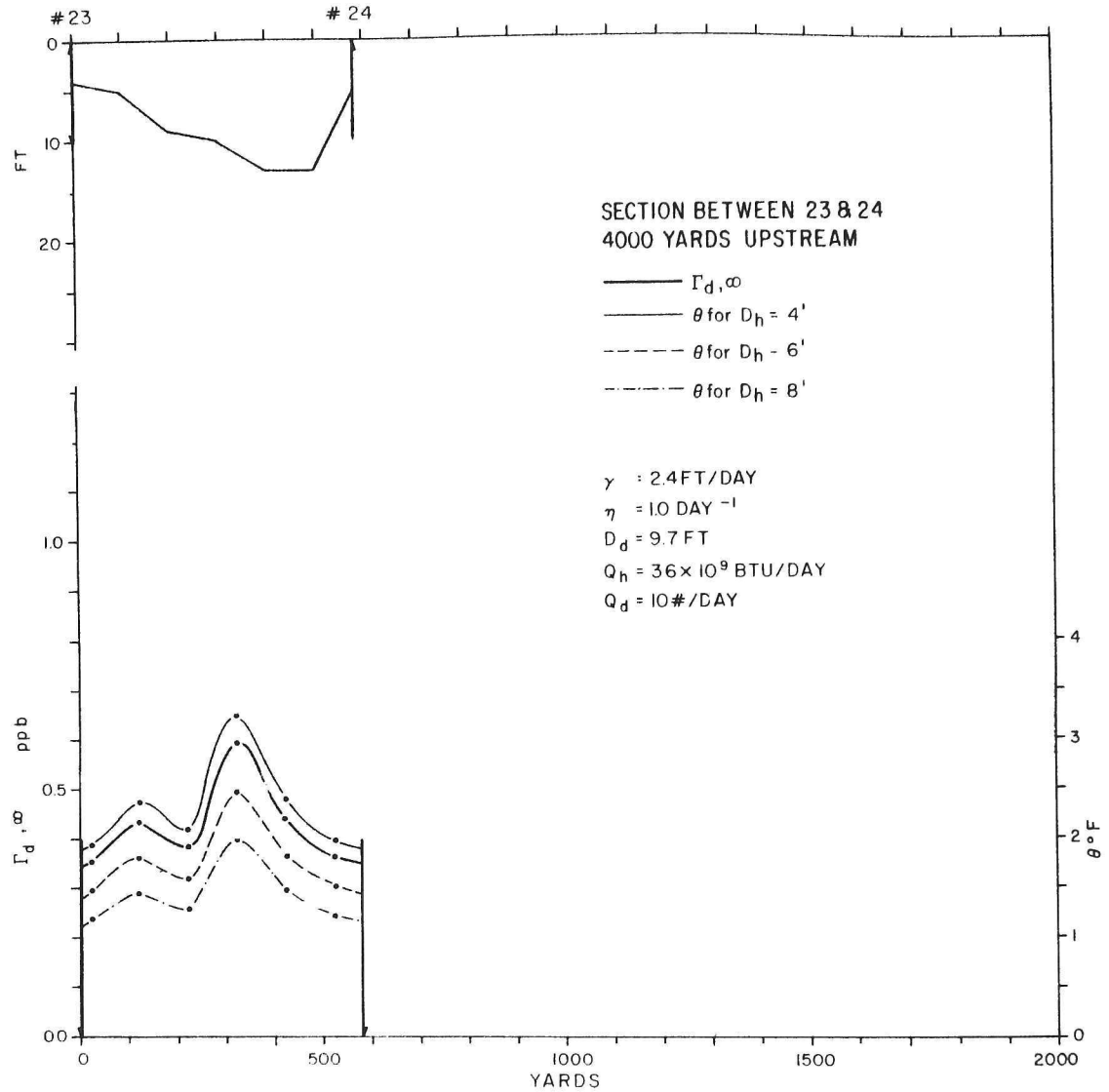

Fig. 13. Observed dye distribution and predicted distribution of excess temperature at section 4000 yd upstream from release point, under steady-state conditions, during flood tide.

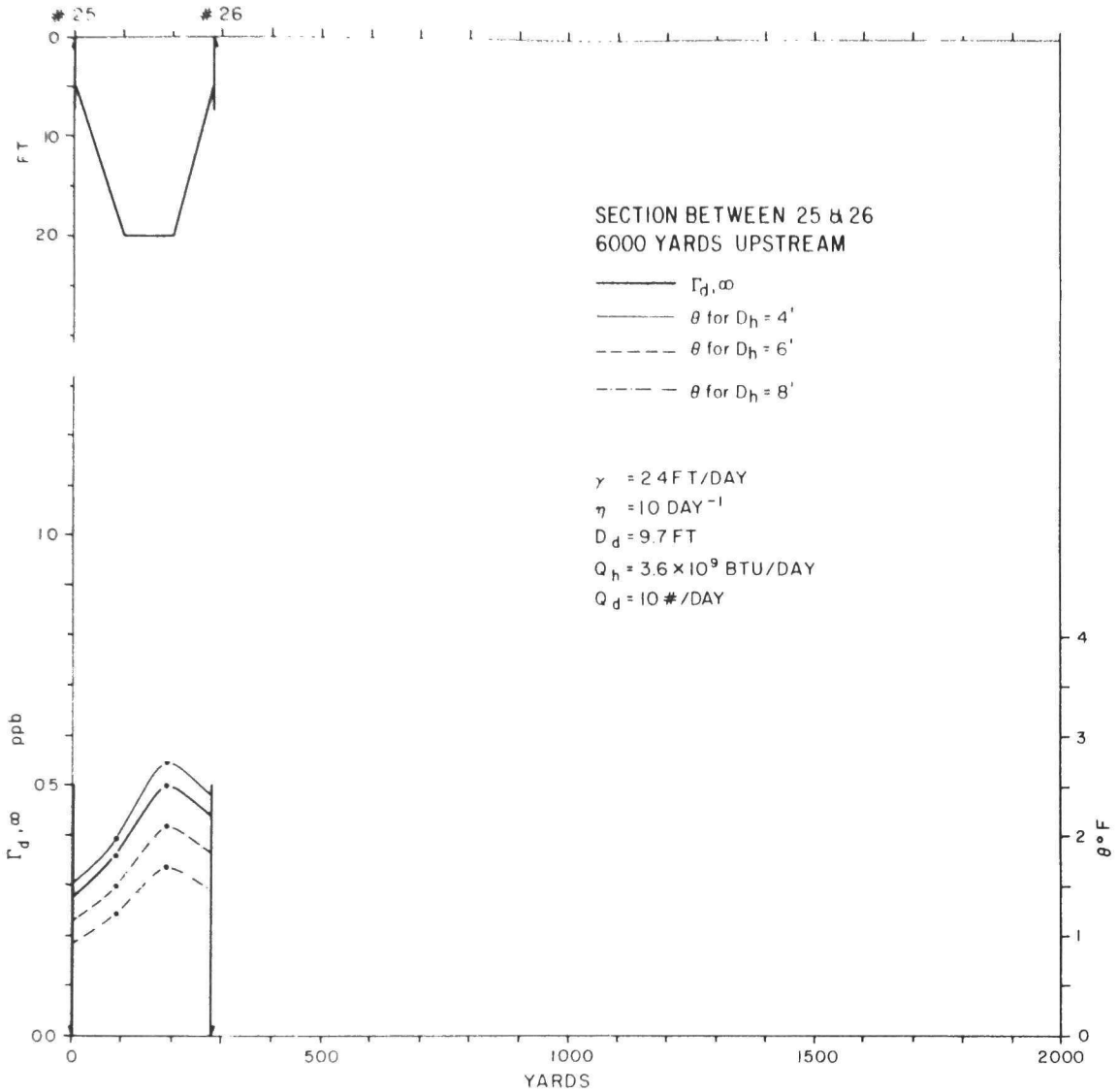

Fig. 14. Observed dye distribution and predicted distribution of excess temperature at section 6000 yd upstream from release point, under steady-state conditions, during flood tide.

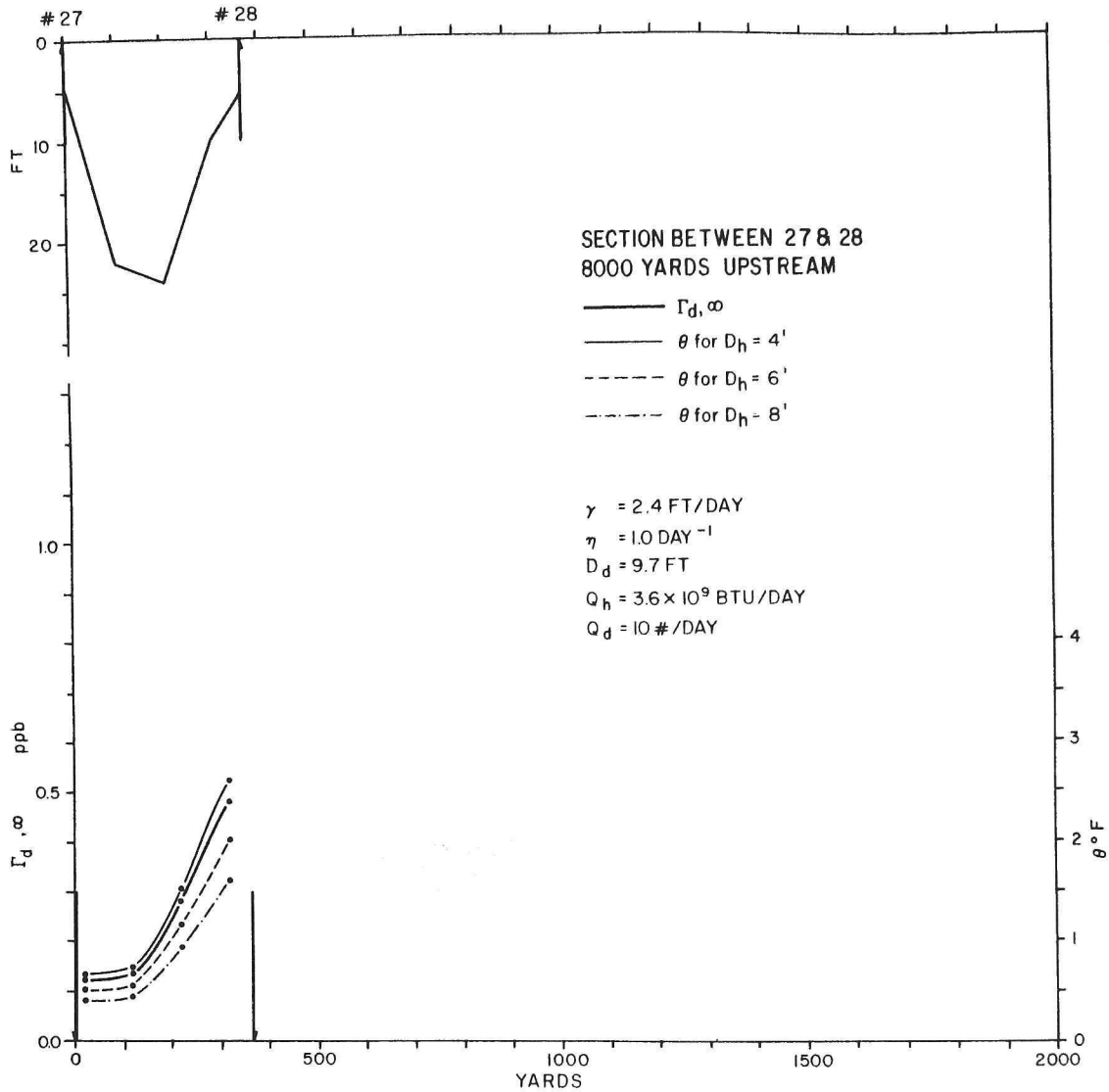

Fig. 15. Observed dye distribution and predicted distribution of excess temperature at section 8000 yd upstream from release point, under steady-state conditions, during flood tide.

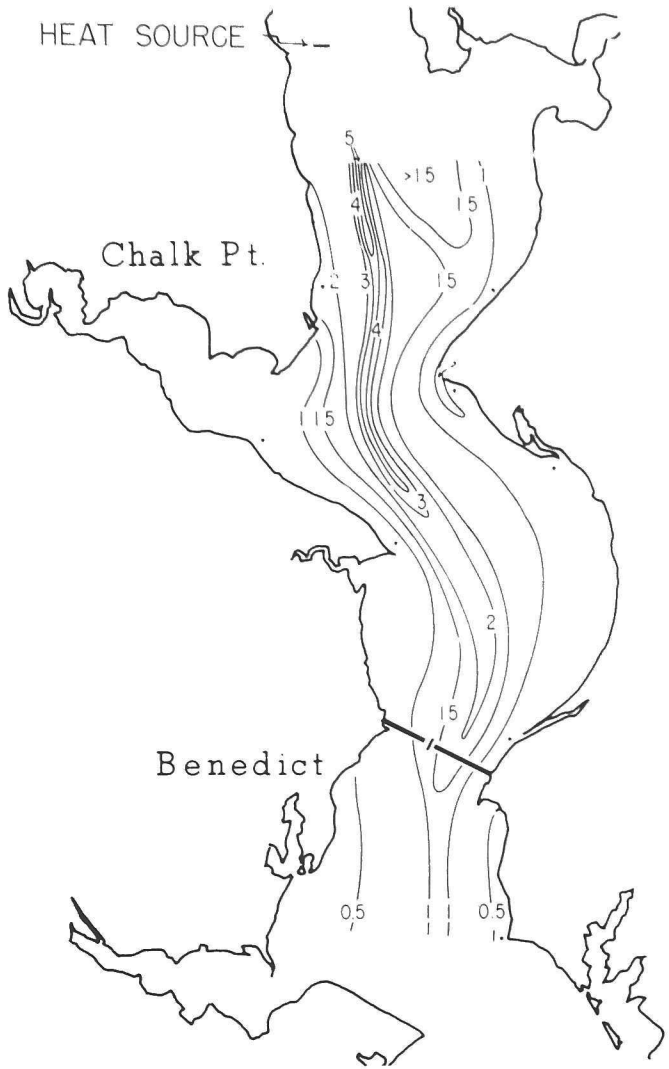

PATUXENT RIVER

Yards

1000 0 1000 2000 3000

EBB

Excess Temp, θ, in °F

D_h = 4 ft

D_d = 8.4 ft.

Q_h = 36×10^9 BTU/day

Q_d = 10 #/day

γ = 2.4 ft./day

η = 1.0 day^{-1}

— = Source

Fig. 16. Horizontal distribution of predicted excess temperature downstream from heat source on ebb tide for an assumed heated layer thickness D_h = 4 ft.

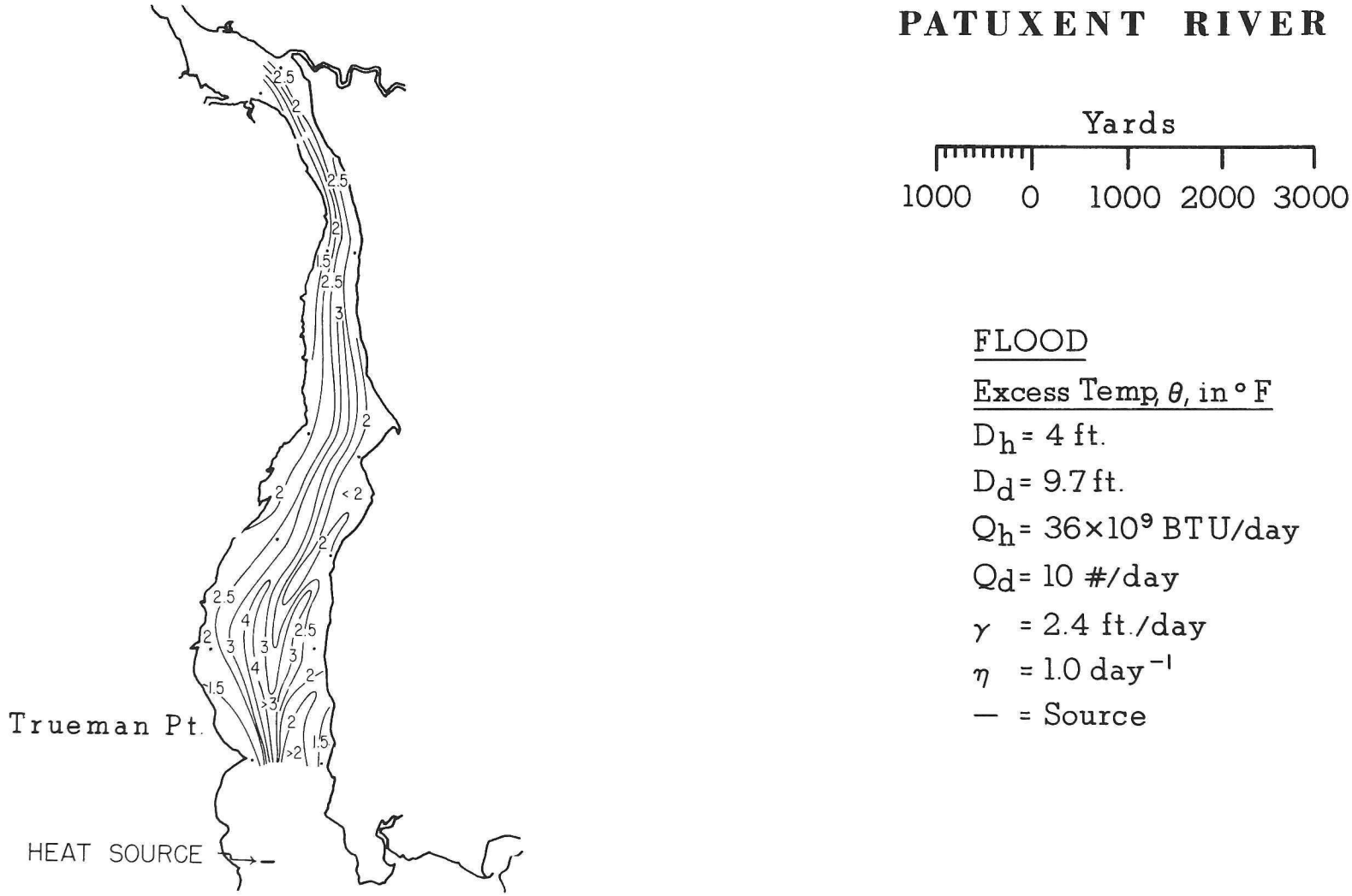

Fig. 17 Horizontal distribution of predicted excess temperature upstream from heat source on flood tide for an assumed heated layer thickness D_h = 4 ft.

APPENDIX

The nonconservative processes of heat loss at the surface

The conservation of heat for a unit volume at the surface of a tidal estuary under natural conditions may be written as:

$$\text{(A-1)}\quad \frac{\partial q_n}{\partial t} = -\frac{\partial}{\partial x_i}(u_i q_n) - \frac{\partial}{\partial x_3}(u_3 q_n) + \frac{\partial}{\partial x_i}\left\{K_{ij}\frac{\partial q_n}{\partial x_j}\right\} + \frac{\partial}{\partial x_3}\left(K_3 \frac{\partial q_n}{\partial x_3}\right) + R \qquad i,j = 1,2$$

where q_n = heat contained in unit volume under natural conditions

u_i = horizontal velocity at a given point (x_i, x_3) at time t

u_3 = vertical velocity at a given point (x_i, x_3) at time t

K_{ij} = the coefficient of eddy diffusion of heat ($K_{ij} = 0$ when $i \neq j$)

R = local time change in heat concentration due to processes of radiation, evaporation, and conduction of sensible heat.

If heat is now added to the estuary by the discharge of condenser cooling water, (A-1) must be rewritten as follows:

$$\text{(A-2)}\quad \frac{\partial q_n'}{\partial t} = -\frac{\partial}{\partial x_i}(u_i q_n') - \frac{\partial}{\partial x_3}(u_3 q_n') + \frac{\partial}{\partial x_i}\left\{K_{ij}\frac{\partial q_n'}{\partial x_j}\right\} + \frac{\partial}{\partial x_3}\left(K_3 \frac{\partial q_n'}{\partial x_3}\right) + R' \qquad i,j = 1,2$$

where the "primes" now refer to the industrialized or heated estuary. It should be noted that (A-2) does not contain a source or sink term, as we are concerned with conditions at a distance removed from the condenser discharge or intake, and their inclusion is not pertinent to the present argument.

Subtracting (A-1) from (A-2) we obtain

$$(A\text{-}3) \quad \frac{\partial q}{\partial t} = -\frac{\partial}{\partial x_i}(u_i q) \quad \frac{\partial}{\partial x_3}(u_3 q) + \frac{\partial}{\partial x_i}\left\{ K_{ij} \frac{\partial q}{\partial x_j} \right\}$$

$$+ \frac{\partial}{\partial x_3}\left(K_3 \frac{\partial q}{\partial x_3}\right) + (R' - R) \qquad i,j = 1,2$$

where $q \equiv q'_n - q_n$ and is the excess heat. In addition, the validity of (A-3) depends upon the eddy coefficients and velocity field being identical under natural conditions and conditions of added excess heat, as do equations (1) and (2) in the basic paper for dye and excess heat.

Let us now examine the last term in (A-3), (R' - R). Both R' and R may be considered as gradients of quantities, f' and f, which are fluxes of heat passing through a unit surface perpendicular to the x_3 (vertical) axis per unit time or

$$(A\text{-}4) \quad (R' - R) \equiv \frac{\partial f'}{\partial x_3} - \frac{\partial f}{\partial x_3} = \frac{\partial (f' - f)}{\partial x_3}$$

Substituting (A-4) in (A-3) we obtain

$$(A\text{-}5) \quad \frac{\partial q}{\partial t} = -\frac{\partial}{\partial x_i}(u_i q) - \frac{\partial}{\partial x_3}(u_3 q) + \frac{\partial}{\partial x_i}\left\{ K_{ij} \frac{\partial q}{\partial x_j} \right\}$$

$$+ \frac{\partial}{\partial x_3}\left(K_3 \frac{\partial q}{\partial x_3}\right) + \frac{\partial (f' - f)}{\partial x_3} \qquad i,j = 1,2$$

It is now assumed that the heated effluent is discharged into the estuary and mixes by advection and diffusion between the surface ($x_3 = \eta$) and a depth D_h (the plane $x_3 = 0$ coincides with the mean tide level). The kinematic boundary condition requires that there be no flux due to advection or eddy diffusion through the top boundary. The terms f' and f involve processes which are primarily restricted to the near vicinity of the air-sea boundary. It may at some later point

become necessary to make further assumptions regarding diffusion and advection at the bottom boundary ($x_3 = D_h$) but for the present it is desired to retain maximum possible generality in our result. The boundary conditions may be expressed as

$$(u_3 q)_\eta = (q)_\eta \frac{\partial \eta}{\partial t}$$

$$(A\text{-}6) \qquad (K_3 \frac{\partial q}{\partial x_3})_\eta = 0$$

$$(f' - f)_{D_h} = 0$$

Integrating (A-5) from $x_3 = 0$ to $x_3 = D_h$ and applying Leibniz' rule together with (A-6) gives

$$(A\text{-}7) \quad \frac{\partial}{\partial t}\int_\eta^{D_h} q\,dx_3 - (q)_{D_h}\frac{\partial D_h}{\partial t} = -\frac{\partial}{\partial x_i}\int_\eta^{D_h}(u_i q)\,dx_3 + (u_i q)_{D_h}\frac{\partial D_h}{\partial x_i}$$

$$- (u_3 q)_{D_h} + \frac{\partial}{\partial x_i}\int_\eta^{D_h} K_{ij}\frac{\partial q}{\partial x_j}\,dx_3$$

$(i,j = 1,2)$

$$- (K_{ij}\frac{\partial q}{\partial x_j})_{D_h}\frac{\partial D_h}{\partial x_i} + (K_3\frac{\partial q}{\partial x_3})_{D_h} - (f' - f)_\eta$$

If we now assume that our estuary is vertically homogeneous throughout the layers $x_3 = \eta$ and $x_3 = D_h$, that is, u_i, q, and K_{ij} are not functions of x_3, (A-7) becomes

$$(A\text{-}8) \quad \frac{\partial}{\partial t}\left[q(D_h - \eta)\right] - (q)_{D_h}\frac{\partial D_h}{\partial t} = -\frac{\partial}{\partial x_i}\left[u_i q(D_h - \eta)\right] + (u_i q)_{D_h}\frac{\partial D_h}{\partial x_i}$$

$$- (u_3 q)_{D_h} + \frac{\partial}{\partial x_i}\left\{K_{ij}\frac{\partial q}{\partial x_j}(D_h - \eta)\right\}$$

$(j,j = 1,2)$

$$- (K_{ij}\frac{\partial q}{\partial x_j})_{D_h}\frac{\partial D_h}{\partial x_i} + (K_3\frac{\partial q}{\partial x_3})_{D_h} - (f' - f)_\eta$$

Applying the equation of continuity to (A-8) gives

$$(A\text{-}9)\quad (D_h - \eta)\frac{\partial q}{\partial t} = -(D_h - \eta)\, u_i \frac{\partial q}{\partial x_i} + (D_h - \eta)\frac{\partial}{\partial x_i}\left\{ K_{ij}\frac{\partial q}{\partial x_j}\right\} + \left(K_3 \frac{\partial q}{\partial x_3}\right)_{D_h} - (f' - f)_\eta \qquad i,j = 1,2$$

Equation (A-9) merely states that the excess heat in our small volume of depth $D_h - \eta$ is changed locally by horizontal advection, horizontal diffusion, vertical diffusion through the bottom, and exchange of sensible heat, radiation, and evaporation through the top.

We may now express the last term on the right-hand side of (A-9) in terms of incoming and outgoing heat fluxes as follows:

$$(A\text{-}10)\quad (f')_\eta = q_s - q_{sr} + q_\ell - q_{\ell r} \cdot q_{\ell b}' - q_e' - q_c'$$

$$(A\text{-}11)\quad (f)_\eta = q_s - q_{sr} + q_\ell - q_{\ell r} - q_{\ell b} - q_e - q_c$$

where

Incoming

q_s = solar short wave radiation incident on water surface

q_ℓ = incoming long wave radiation from atmosphere

Outgoing

q_{sr} = reflected short wave solar radiation from water surface

$q_{\ell r}$ = reflected long wave radiation from water surface

$q_{\ell b}$ = long wave radiation from water surface

q_e = amount of heat energy utilized by evaporation

q_c = heat energy conducted from surface as sensible heat

The q's represent heat flux through a unit surface per unit time. The "primes" in (A-10) and (A-11) again refer to the heated estuary. Note that the first four terms on the right side of (A-11) are the same as the corresponding terms in (A-10).

Substituting (A-10) and (A-11) in (A-9) we obtain

$$(A\text{-}12)\quad \frac{\partial q}{\partial t} = - u_i \frac{\partial q}{\partial x_i} + \frac{\partial}{\partial x_i}\left\{ K_{ij} \frac{\partial q}{\partial x_j} \right\} + \frac{1}{D_h - \eta} \left(K_3 \frac{\partial q}{\partial x_3}\right)_{D_h}$$
$$- \frac{1}{D_h - \eta} \left[(q_{\ell b}' - q_{\ell b}) + (q_e' - q_e) + (q_c' - q_c) \right]_\eta \qquad i,j = 1,2$$

It can be shown that $(q'_{\ell b} - q_{\ell b})$ and $(q'_c - q_c)$ can be expressed as functions of the temperature difference between heated and natural conditions and $(q'_e - q_e)$ as a function of the vapor pressure difference or

$$(A\text{-}13)\quad \left[(q_{\ell b}' - q_{\ell b}) + (q_e' - q_e) + (q_c' - q_c) \right]_\eta = 1.10\,(T_h - T_n) + 13.0\,W(e_h - e_n)$$
$$+ 0.132\,W(T_h - T_n)$$

where T_h = water temperature in degrees F under conditions of added excess heat

T_n = water temperature in degrees F under natural conditions

W = wind speed in mph at an elevation of 26 ft

e_h = vapor pressure of saturated air at temperature T_h, in inches of Hg

e_n = vapor pressure of saturated air at temperature T_n, in inches of Hg.

(A-13) may be simplified if we approximate the vapor pressure difference $(e_h - e_n)$ by the following expression:

(A-14) $(e_h - e_n) \doteq \beta\,(T_h - T_n)$

where β is assumed to be a constant. The effect of this assumption will be examined later. Upon combining (A-12), (A-13), and (A-14), we obtain

$$\text{(A-15)}\quad \frac{\partial\theta}{\partial t} = -\,u_i\,\frac{\partial\theta}{\partial x_i} + \frac{\partial}{\partial x_i}\left\{K_{ij}\,\frac{\partial\theta}{\partial x_j}\right\} + \frac{1}{(D_h-\eta)}\,(K_3\,\frac{\partial\theta}{\partial x_3})_{D_h} - \frac{1}{(D_h-\eta)}\cdot\frac{\xi\theta}{\rho e} \qquad i,j = 1,2$$

where $\xi = 1.10 + 13.0\,\beta W + 0.132\,W$

$\theta = T_h - T_n = q/\rho c$

ρ = density

c = specific heat.

Finally, if we replace $\xi/\rho c$ by γ and $D_h - \eta$ by D_h, (A-15) gives

$$\text{(A-16)}\quad \frac{\partial\theta}{\partial t} = -\,u_i\,\frac{\partial\theta}{\partial x_i} + \frac{\partial}{\partial x_i}\left\{K_{ij}\,\frac{\partial\theta}{\partial x_j}\right\} + \frac{1}{D_h}\,(K_3\,\frac{\partial\theta}{\partial x_3})_{D_h} - \frac{\gamma\theta}{D_h} \qquad i,j = 1,2$$

Let us consider for the moment just the term in (A-16) which represents loss of excess heat to the atmosphere at the air-sea boundary per unit time (i.e., cooling). We can write

$$\text{(A-17)}\quad \left[\frac{\partial\theta}{\partial t}\right]_{\text{cooling}} = -\,\frac{\gamma\theta}{D_h}$$

If it is assumed that D_h and γ are not functions of time, (A-17) is integrable over a time period t, and gives

$$\text{(A-18)}\quad \theta_t = \theta_o \exp\left(-\,\frac{\gamma}{D_h}\,t\right)$$

where θ_t = value of excess temperature at time t

θ_o = initial value of excess temperature .

(A-18) may also be written as

$$(A\text{-}19) \quad \Gamma_h(t) = \Gamma_h(o) \exp\left(-\frac{\gamma}{D_h} t\right)$$

Thus it is seen that the effect of cooling is an exponential decrease in excess temperature or heat with time, subject to the boundary conditions and assumptions applied. It should be noted that D_h is not a function of time but may be a function of x_1 and x_2 for the model selected.

Table 1 shows values of γ computed for wind velocities of 5 mph

Table 1

γ (ft hr^{-1}) as a function of wind velocity, and of T_h and T_n

		T_h						
	T_n	70	75	80	85	90	95	100
W = 5 mph	65°	0.052	0.054	0.056	0.059	0.060	0.063	0.067
	70°	---	0.057	0.059	0.060	0.063	0.067	0.070
	75°	---	---	0.060	0.063	0.065	0.068	0.071
	80°	---	---	---	0.065	0.068	0.071	0.075
W = 10 mph	65°	0.086	0.091	0.094	0.100	0.105	0.111	0.117
	70°	---	0.097	0.098	0.105	0.108	0.114	0.121
	75°	---	---	0.104	0.108	0.113	0.119	0.125
	80°	---	---	---	0.113	0.119	0.125	0.132

and 10 mph using the values of β determined by the various values of $(T_h - T_n)$. Earlier it was assumed that $(e_h - e_n)$ varies linearly with $(T_h \; T_n)$. It was to evaluate the effect of this assumption (β constant), that γ was computed. It is seen that for any given T_n the variation in γ with T_h, or θ, over a range of 35 F is equivalent to the variation in γ which would be produced by a wind variation of 2 mph. Since it is doubtful whether W can be estimated to ±2 mph with any certainty, it is considered sufficient to assume γ constant for any given application.

To summarize, equation (A-16) has been developed; it describes the local rate of change of excess temperature in terms of the physical processes of advection and diffusion and the process of cooling. The cooling process leads to an exponential decrease in excess temperature with time, which is described by equation (A-18) or (A-19). The form of the relationship shown in equation (A-18) or (A-19) has previously been proposed by Gameson et al (1959)*. They report experimentally determined values of γ ranging from 2.6 cm hr^{-1} for a stream to 3.7 cm hr^{-1} for the Thames estuary under various weather conditions. In our units, these correspond to values of 0.09 to 0.12 ft hr^{-1}, respectively.

---

* Gameson, A.L.H., J.W. Gibbs, and M.J. Barrett (1959) A preliminary temperature survey of a heated river: Water and Water Engineering, January 1959; reprint no. 336 from Water Pollution Research Laboratory, Stevenage, Herts., England.

Derivation of equation (4)

Let $h_c(t)$ = concentration of excess heat of a moving infinitesimal volume of depth D_h and unit cross-sectional area, at time t after release of a single infinitesimal source of strength m, under conditions when both the physical processes of dispersion and heat losses due to cooling are taken into account

$h_o(t)$ = concentration of excess heat of a moving infinitesimal volume of unit cross-sectional area and depth D_h, at time t after release of a single infinitesimal source of strength m, under conditions of no heat loss due to cooling (i.e., only the physical process of dispersion acts to change the concentration of excess heat)

Q_n = the rate of release of excess heat from a continuous source which is thought of as being composed of a large number of instantaneous releases of strength m at the rate N day^{-1}.

The budget of excess heat at position x_i for a single release of strength m for our small volume is identical with (A-16) if we replace θ by $h_c(t)$. Thus

$$\text{(A-20)}\quad \frac{\partial h_c(t)}{\partial t} = - u_i \frac{\partial h_c(t)}{\partial x_i} + \frac{\partial}{\partial x_i}\left\{ K_{ij} \frac{\partial h_c(t)}{\partial x_j} \right\} + \frac{1}{D_h}\left\{ K_3 \frac{\partial h_c(t)}{\partial x_3} \right\} D_h - \frac{\gamma h_c(t)}{D_h} \qquad i,j = 1,2$$

subject, of course, to the same assumptions and boundary conditions as

before.

Similarly, we can write

$$\text{(A-21)}\quad \frac{\partial h_o(t)}{\partial t} = - u_i \frac{\partial h_o(t)}{\partial x_i} + \frac{\partial}{\partial x_i}\left\{ K_{ij} \frac{\partial h_o(t)}{\partial x_j} \right\} + \frac{1}{D_h}\left\{K_3 \frac{\partial h_o(t)}{\partial x_3}\right\} D_h$$

$$i,j = 1,2$$

By inspection of (A-20) and (A-21), $h_c(t)$ and $h_o(t)$ are related by

$$\text{(A-22)}\quad h_c(t) = h_o(t) \exp\left(- \frac{\gamma}{D_h} t\right)$$

If we now multiply (A-20) by Ndt where $N = Q_h/m$, and integrate from t = 0 to time t, we obtain

$$\text{(A-23)}\quad Nh_c(t) = - \int_o^t Nu_i \frac{\partial h_c(t)}{\partial x_i} dt + \frac{\partial}{\partial x_i} \int_o^t NK_{ij} \frac{\partial h_c(t)}{\partial x_j} dt + \frac{1}{D_h} \int_o^t \left\{K_3 \frac{\partial h_c(t)}{\partial x_3}\right\} D_h N dt - \frac{\gamma}{D_h} \int_o^t Nh_c(t)dt \quad i,j = i,2$$

If (A-16) is now expressed in terms of $\Gamma_h(t)$ (due to a continuous source Q_h) instead of θ and compared term for term with (A-23), it can readily be seen that they are identical if

$$\text{(A-24)}\quad \int_o^t Nh_c(t)dt = \Gamma_h(t)$$

and if K_{ij}, K_3, and u_i are not functions of time. That is, a continuous source may be considered to be a superposition of instantaneous releases of strength m at the rate N, subject to (A-24) and the lack of time dependence of the eddy coefficients and the horizontal velocity field. This latter restriction is not too critical if one considers that in

the basic reduction of the concentration data, concentrations measured at approximately identical phases of the tide are utilized.

Differentiating (A-24) with respect to t, we obtain

$$Nh_c(t) = \frac{\partial \Gamma_h(t)}{\partial t} \tag{A-25}$$

By a similar line of reasoning

$$\int_0^t Nh_o(t)dt = \Gamma_{h,o}(t) \tag{A-26}$$

or

$$Nh_o(t) = \frac{\partial \Gamma_{h,o}(t)}{\partial t} \tag{A-27}$$

Combining (A-22), (A-25), and (A-27) we obtain

$$\frac{\partial \Gamma_h(t)}{\partial t} = \frac{\partial \Gamma_{h,o}(t)}{\partial t} \cdot \frac{h_c(t)}{h_o(t)} = \frac{\partial \Gamma_{h,o}(t)}{\partial t} \exp\left(-\frac{\gamma}{D_h} t\right) \tag{A-28}$$

which is the required equation (4).